

THE PREDICTIVE CAPABILITY OF FAILURE MODE CONCEPT - BASED STRENGTH CRITERIA FOR MULTIDIRECTIONAL LAMINATES

R.G. Cuntze* and A. Freund (student)

*Prof. Dr.-Ing. habil. Ralf G. Cuntze, Main Department 'Analysis', MAN Technologie AG, Liebigstraße 5a, D-85757 Karlsfeld, Germany; Tel.: 0049 8131 89-1783, Fax: -1939, E-mail: Ralf_Cuntze@mt.man.de

Abstract

This contribution is a postrunner to the 'failure exercise'. It focuses on two aspects of the theoretical prediction of failure in composites¹⁻⁴: First, the derivation of failure conditions for a unidirectional (UD) lamina with the prediction of initial failure of the embedded lamina and secondly, the treatment of nonlinear, progressive failure of 3-dimensionally stressed laminates until final failure. The failure conditions are based on the so-called Failure Mode Concept (FMC) which takes into account the material-symmetries (by the application of invariants) of the UD-lamina homogenized to a 'material', and on a strict failure mode thinking.

The results of the investigation are stress-strain curves for the various given GFRP-/CFRP-UD-laminae, biaxial failure stress envelopes for the UD-laminae, and initial as well as final biaxial failure envelopes for the laminates. In addition a brief comparison ~~of~~ between Puck's ~~with~~ and Cuntze's failure theory is presented by the authors themselves.

Keywords: multiaxial stressing, nonlinear behaviour, multidirectional laminates

NOTATION

In the notation, self-explaining symbols are used if a property is addressed. A lamina (is defined to be the calculation unit) may consist of several physical layers.

Unidirectional lamina

a_s, b_s : Ramberg/Osgood parameters in softening regime

$b_{\perp}^{\tau}, b_{\perp\parallel}, b_{\perp\parallel}^{\tau}$: Curve parameters

$E_1 = E_{\parallel}, E_2 = E_3 = E_{\perp}$: Elastic moduli of a UD lamina in the directions x_1, x_2, x_3

$E_{1(\text{tan})}, E_{3(\text{sec})}$: A tangent and a secant elastic modulus

$\text{Eff}^{(\text{res})}$: Resultant stress effort of all interacting failure modes. Corresponds to Puck's exposure factor f_E

$\text{Eff}^{(\text{mode})}$: Stress Effort of a UD-lamina in a failure mode, eg $\sigma_{\text{eq}}^{\parallel\tau} / R_{\parallel}^c = \text{Eff}^{\parallel\tau}$. Corresponds to $1/f_{\text{Res}}^{\parallel\tau}$ if linear behaviour

$\text{maxEFF}^{(\text{mode})}$: Stress Effort of the maximum stressed failure mode

$e_{\parallel}^t, e_{\parallel}^c$: Tensile and compressive failure strain of a UD-lamina in x_1 direction

$F_{\parallel}^{\sigma}, F_{\parallel}^{\tau}, F_{\perp}^{\sigma}, F_{\perp}^{\tau}, F_{\perp\parallel}$: Failure functions for FF and IFF

$f_{\text{Res}}^{(\text{mode})}$: Reserve factor = stretching factor for the applied stress state necessary to achieve the failure stress state of the mode, eg $f_{\text{Res}}^{\perp\sigma} = R_{\perp}^t / \sigma_{\text{eq}}^{\perp\sigma} = 1$

f_E : Stress exposure factor of Puck

$f_{\text{Res}}^{(\text{res})}$: Resultant reserve factor of all interacting failure modes

$G_{21}, G_{21(\text{sec})}$: Shear modulus of a UD lamina in the x_2, x_1 direction; secant shear modulus

I_1, I_2, I_3, I_4, I_5 : Invariants of the transversally-isotropic UD-material

MS: Margin of Safety = $f_{\text{Res}} - 1$

m : Mode interaction coefficient

$R_{p0.2}$: Stress value at 0.2 % plastic strain

$R_{\parallel}^t \equiv X^t, R_{\parallel}^c \equiv X^c$: UD tensile and compressive (basic) strength parallel to the fibre direction

$R_{\perp}^t \equiv Y^t, R_{\perp}^c \equiv Y^c$: UD tensile and compressive strength transverse to the fibre direction

$R_{\perp\parallel} \equiv S$: Shear strength of a UD lamina transverse/parallel to the fibre direction

v_f : volume fraction

x_1, x_2, x_3 : Coordinate system of a unidirectional (UD-)lamina (x_1 = fibre direction, x_2 = direction transverse to the fibre, x_3 = thickness direction)

$\varepsilon_1, \varepsilon_2, \varepsilon_3$: Normal strains of a unidirectional lamina

ν_{12} : Major Poisson's ratio in the 'failure exercise' (corresponds to $\nu_{\perp\parallel}$ in the German guideline VDI 2014. There is no rationale for ν_{12} or ν_{21} . In the early times the application of ν_{21} was preferred because this denotation makes more sense (location first, cause second))

$\sigma_1, \sigma_2, \sigma_3$: Normal stresses in a unidirectional layer

σ_1^c, σ_2^t : Compressive stress, a tensile stress in fibre direction

$\sigma_{\parallel}, \sigma_{\perp}$: Stresses parallel and transverse to the fibre direction

$\hat{\sigma}, \hat{\tau}$: Laminate mean stresses

$\{\sigma\}_{(L)}, \{\sigma\}_{(R)}$: Load-dependent stresses; residual stresses

$\sigma_{\text{eq}}^{(\text{mode})}$: Equivalent stresses of a mode ($\sigma_{\text{eq}}^{\parallel\sigma}, \sigma_{\text{eq}}^{\parallel\tau}, \sigma_{\text{eq}}^{\perp\sigma}, \sigma_{\text{eq}}^{\perp\tau}, \sigma_{\text{eq}}^{\perp\parallel}$), includes load stresses and residual stresses

$\tau_{12} = \tau_{21}, \tau_{13} = \tau_{31}, \tau_{23} = \tau_{32}$: Shear stresses of a unidirectional lamina in the elastic symmetry directions. The first subscript locates the direction normal to the plane on which the shear stress is acting; the second subscript indicates the direction of the shear force

$\tau_{\perp\parallel}, \tau_{\perp\perp}$: Shear stressing transverse/parallel and transverse/transverse to the fibre direction

$\gamma_{12} = \gamma_{21}; \gamma_{13} = \gamma_{31}; \gamma_{23} = \gamma_{32}$: Shear strains of a unidirectional layer.

Characteristics of the fibres

E_{1f} : Elastic modulus in x_1 direction

σ_{1f}, σ_{2f} : Stress in x_1 direction; stress in x_2 direction.

Potential fracture plane (for the comparison Puck - Cuntze)

$R_{\perp}^{(+)\text{A}}, R_{\perp}^{(-)}$: Fracture resistance of the action plane against its fracture due to transverse tensile and compression stressing. They correspond to strength values R_{\perp}^t, R_{\perp}^c .

$R_{\perp\parallel}^{\text{A}}$: Fracture resistance of the action plane against its fracture due to transverse/parallel shear stressing := $R_{\perp\parallel}$

$R_{\perp\perp}^{\text{A}}$: Fracture resistance of the action plane against its fracture due to transverse/transverse shear stressing

~~$R_{\perp\perp}^{\text{A}}$: Fracture resistance of the action plane against its fracture due to transverse/transverse shear stressing~~

x_1, x_n, x_t : Coordinate system rotated with respect to the fibre direction by an angle θ from the x_2 direction to the x_n direction

σ_n , τ_{nt} , τ_{nl} : Normal stress, normal/longitudinal shear stress, normal/transverse shear stress acting on the potential fracture plane (Mohr-Coulomb stresses)

θ : Angle between the x_2 axis and the x_n axis

θ_{fp} : Angle of the fracture plane.

Abbreviations

CLT: Classical Laminate Theory

CoV: Coefficient of Variation

DLL: Design Limit Load

F : Failure function

FEA: Finite Element Analysis

FF : Fibre Failure

FMC: Failure Mode Concept

FoS : Factor of Safety

FPF : First Ply Failure

FRP : Fibre-Reinforced Plastic

IFF : Inter-Fibre Failure

MS : Margin of Safety

Indices, signs

A : indicates an Action plane quantity

c, t : compression, tension (German Guideline VDI 2014)

f, m : fibre, matrix

fp : fibre-parallel fracture plane

(sec) : secant modulus

(res) : resultant

s : symmetric lay-up, softening

Res : Reserve

\wedge : laminate mean stress or average stress of laminate

(+), (-) : mathematical notations for tension and compression

- --- : statistical mean

τ , σ : indicate the failure induced by the normal or shear Mohr stress

1 INTRODUCTION

For a reliable *Strength Proof of Design* of a laminate composed of UD-laminae reliable failure criteria and a reliable progressive failure analysis are needed.

The nonlinear behaviour of laminates composed of *brittle* laminae (these are the materials in the 'failure exercise') originates from the damage development around inherent defects in the constituent matrix and at the interface fibre-matrix (ductile matrix materials would show necking and so-called crazing ,appears as whitening, in a tensile test). These defects grow to microcracks and later to cracks under increased stressing. Therefore, ***the usually in the 'plasticity theory' to be applied global yield failure condition*** (which would need to be anisotropic here) ***is to be replaced by fracture conditions***. Also, ***the*** so-called associated ***flow rule*** (Normality criterion: The subsequent failure surface is indicated by a vector normal to the actual global yield failure surface) ***is replaced by the idea of proportional stressing, that means, the surface increases in the direction of the actual stressing which is seldom the normal direction***. *Partial* mode-related fracture surfaces will confine the subsequent *global* anisotropic yield surface piecewise. These fracture surfaces are essentially described by those fracture conditions for the UD lamina (defined here to be the material the laminate consists of) which are matrix-dominated.

The development of UD failure criteria and of degradation models for the progressive failure analysis gave rise to activities in Germany. These activities concentrated as far as possible on the improvement of failure criteria and their verification by multiaxial testing with the existing specimens and test rigs⁵⁻¹¹.

Since 1980 a group close to A. Puck has tried to improve Puck's 'old' criteria^{8,9} which already distinguished between the two failure types, fibre failure (FF) and inter fibre failure (IFF). In 1992, A. Puck¹² eventually established his 'new' set of IFF-criteria following an idea, proposed 1980 by Z. Hashin¹³, which was based on a modified Mohr/Coulomb theory.-

From 1992⁸ to 1997, R. Cuntze¹⁴ as well as others¹⁵⁻²² focussed on the *Puck/Hashin IFF-Strength Criteria*, which are based on the determination of the fracture plane. The result of this work was incorporated in the final report of a research project⁶. In parallel, since 1994 Cuntze has investigated invariant-based formulations of strength criteria for isotropic and anisotropic materials²³⁻²⁹. Cuntze's main idea is not the basement on invariants but the strict allocation of a strength criterion to one failure mode and to one associated basic strength.

While Cuntze was studying the invariant-based v. Mises yield criterion – it describes one (strength) failure mode, the 'shear yielding', and allows for the determination of the slip line angles – the question raised to him: Why should it not be possible to formulate for each single failure mode of an anisotropic material an appropriate invariant-based *mode failure criterion* which might probably (a further condition has to be applied) later allow for post-determination of the failure angle, if desired?

The application of invariants is almost standard for isotropic materials. However there, the main intention is to build up a yield criterion (this means for one failure mode or one phenomenon) or a *global* fracture criterion that includes all fracture failure modes occurring in the isotropic case. Such a global criterion has on the one hand numerical advantages because one has to apply only one criterion, but on the other hand, it may lead to erroneous results due to its physical shortcoming because it tries to map *several* failure modes).

Invariant-based failure criteria have been formulated for a large number of isotropic materials. As the first Z. Hashin¹³ seems to have postulated (1980) in the same paper, in parallel to his 'Mohr-Coulomb model'-based IFF criteria, invariant-based *UD-failure criteria*. Based on curve fitting consideration and not on physical reasoning, Hashin chose a quadratic approximation which reads in its general form ~~However, he did not follow consequently this way.-~~

$$A_1 I_1 + B_1 I_1^2 + A_2 I_2 + B_2 I_2^2 + C_{12} I_1 I_2 + A_3 I_3 + A_4 I_4 = 1 \quad ,$$

and which includes six strengths (for the definition of the invariants, see (Has80)¹³).

From the 3D failure criterion above he modeled four distinct failure modes: the tensile and compressive fibre modes and two matrix modes. This results in piecewise smooth failure surfaces which do not fit well (fig.3 in¹³). The comparison of Cuntze's results²⁹ with Hashin's formulations show some differences: 1) Hashin's choice of a single quadratic approximation, 2) two matrix modes, 3) six strengths (Hashin in reality uses $R_{\perp\perp}$ (not Puck's $R_{\perp\perp}^A$) which is identical to the strength R_{\perp}^t in our actual case of brittle behaviour), and 4) the application of *tensile* stress σ_1 combined with longitudinal shear stress τ_{21} (not just the fibre tensile stress alone as with Cuntze or Puck). Only for fibre parallel compression failure Cuntze considers such a contribution of the longitudinal shear stress. But, due to insufficient data for this *compression* FF also the simple maximum stress criterion is proposed by Cuntze, like Hashin.

Since the early eighties J. P. Boehler^{30,31} et al. eventually extensively pursued the idea of applying invariant-based criteria which they had partly verified by test. Because this working group did not present the criteria in the conventional UD stresses, their valuable results unfortunately did not attract the 'stress man'.

Of course, also Tsai/Wu's polynomial failure conditions may be transformed into formulations of invariant terms.

Later in 1996 Cuntze influenced R. Jeltsch-Fricker and S. Meckbach from the University of Kassel to pick up the idea of invariant-based formulations ~~criteria, the results of which can now be found in several papers^{28, 33}~~. They approximated the 'Puck/Hashin IFF body' by means of two invariant formulations^{32,33}.

The idea of thinking in strength failure modes is not a new idea, but the so-called Failure Mode Concept (FMC) more strictly applies the 'mode thinking' and more consequently uses the advantage of formulating the failure conditions (*interaction of stresses within a mode*) by the *material symmetries respecting invariants*, which contain the lamina stresses of the FEM output. This approach, according to the number of the material symmetries, requires two independent FF modes and three IFF modes. The application to UD material is the most intensive application of Cuntze's FMC, which is claimed to be applicable to any material^{23,26,27}. Each of Cuntze's five (see also Christensen³⁴) failure modes is characterized by one strength and one modulus.

The choice of the invariants in Cuntze's FMC is supported by physical consideration based upon Beltrami. The decision for an individual basic invariant is directed by the fact whether the material element is subjected in the envisaged failure mode to a volume change or a shape change.

Cuntze's previous experience with structural reliability^{19,35-38}, where failure mode thinking is a basic idea, helped to simply model the *interaction of modes* within a lamina by the application of a spring model.

Cuntze tries to formulate easy-to-handle homogeneous invariant-based criteria with stress terms of the lowest possible order and which make a search of the fracture plane not necessary. ~~of the action~~ The FF criteria are treated as decoupled from the IFF ones. The interaction of FF with IFF is considered probabilistically as within the IFF modes by the spring model mentioned above.

Confronted with various questions of the 'UD failure criteria community', R. Cuntze in cooperation with A. Puck tries to outline in this contribution (see Annex 1) the coincidences and main differences of their IFF theories:

A. Puck's approach uses –as proposed by Hashin– a modified Mohr/Coulomb³⁹ theory for brittle IFF of unidirectional (transversally-isotropic) laminae. For IFF thereby is an automatic interaction of stresses included due to basing IFF just on the three so-called 'action plane stresses ($\sigma_n, \tau_{nt}, \tau_{nl}$)'. These stresses have a common action plane (Fig.A1/3). Therefore, these criteria are called 'action plane strength criteria'. Puck discriminates two fundamental regimes: $\sigma_n > 0$ and $\sigma_n < 0$. The unknown IFF fracture angle is determined when the action *plane of maximum stress effort* is 'found'. The well-known conventional global criteria apply all six stresses of the UD lamina and do not take into consideration whether they might act on the same or on different action planes.

~~H~~–It is very simple in the 'plasticity theory of isotropic materials' to develop a so-called 'single *yield* failure surface' criterion, that means *one* global criterion, due to the existence of only one failure phenomenon, the isotropic yielding. A global criterion for *fracture* may include more than one fracture failure mode potentially occurring under the various stress states. It is sometimes also used instead of a global *yield* criterion in spite of the facts that it only confines a global yield surface (yield capacity exhausted) and that it generates a different shape.

And for laminae? For them, as already mentioned, instead of a matrix–determined anisotropic global yield criterion a set of fracture criteria on lamina level is applied. These show due to their various failure modes a 'multifold nonlinearity' requiring much more effort. A further shortcoming is: A set of failure criteria instead of one global one prevents from a simple

implementation into a commercial FEM code in order to take advantage of the code's solution architecture and pre-/postprocessor capabilities (This point waits for being tackled).

Progressive failure analysis⁵⁸⁻⁶⁰ of laminates or the prediction of laminate behaviour up to fracture is the major challenge compared to the derivation of reliable UD-failure criteria. Cuntze assumes a so-called *effective stress-strain curve* for the lamina which respects the influence of being embedded^{29,40} in the laminate.

To be utilized in the nonlinear analysis is the secant modulus which alters for a nonlinear stress-strain curve. However, data are not only needed for the pure failure mode domains but for the *mode interaction domains*, too, where the actual stress state affects more than one mode. The influence of the stress state in a mode interaction domain on the secant modulus of each affected mode is considered by a 'triggering approach'. This approach increases the *equivalent stress* (which considers *all* influencing stresses) *of the affected mode* (~~the secant modulus becomes smaller~~) in the case of *hardening* (the secant modulus becomes a little smaller) and decreases the equivalent stress in the case of *softening* (the secant modulus becomes smaller, too) ~~in the case of softening~~. The mode's *equivalent stress-strain curve* shall be identical with the *uniaxial stress-strain curve* measured.

A crucial difference between Puck's⁴² approach and Cuntze's approach is the treatment of degradation in the non-linear-analysis of the laminate. Both theories apply the self-correcting secant modulus method, however, describe the successive degradation (the softening) differently as well as the rounding-off in the interaction domains of FF and IFF modes.

In the FF-IFF mode interaction domains Puck applies a weakening factor (depending on σ_1) reasoning that single filament failures have a weakening effect on the resistance against IFF. Cuntze automatically respects this fact by the rounding-off procedure. For more information on the differences and coincidences of Puck's and Cuntze's failure theory, see Annex A1.

The *theoretical* background of the following contribution can also be found in the DURACOSYS 99 paper 'Progressive failure of 3D-stressed laminates: Multiple nonlinearity treated by the failure mode concept (FMC)²⁹.

The authors hope to add, with this lamina stress-based *engineering approach*, a 'physically'-based 3D phenomenological model.

2 MAIN FEATURES OF THE FAILURE MODE CONCEPT (FMC)

The features of the FMC are briefly summarised in Table 1. Additional aspects are collected in Table 2—. These features and some further aspects will be described in the coming sections in more details.

3 BASICS

• State of stress:

For the unidirectional (UD) material element Figure 1 depicts the prevailing 3D-state of stress. Additionally, with respect to the symmetries of this transversally-isotropic material (modelled an ideal crystal^{23,26,34}), the 5 basic strengths and 5 elasticities are given (Lekhnitski). A UD-lamina in reality is a low-scale structure with the constituents fibre, matrix and interphase (at the interface). After homogenization it may be called 'material'.

• Invariants:

Strength criteria or failure conditions may be formulated by invariants based on the UD-stresses, see (Boe85³⁰, Has80¹³). Invariants have the advantage that the formulations do not depend on coordinate-system transformations.

From the variety of invariants the following forms were chosen to best describe the multiaxial

behaviour of the material (the numbering of the invariants is different in the various literature, eg., $I_3^{\text{Boehler}} = I_4^{\text{Hashin}}$ and $I_5^{\text{Hashin}} = -\sigma_2 \tau_{31}^2 - \sigma_3 \tau_{21}^2 + 2\tau_{23} \tau_{31} \tau_{21}$).

$$\begin{aligned} I_1 &= \sigma_1; & (\text{Boehler}) \\ I_2 &= \sigma_2 + \sigma_3; \\ I_3 &= \tau_{31}^2 + \tau_{21}^2; \\ I_4 &= (\sigma_2 - \sigma_3)^2 + 4\tau_{23}^2; \\ I_5 &= (\sigma_2 - \sigma_3)(\tau_{31}^2 - \tau_{21}^2) - 4\tau_{23} \tau_{31} \tau_{21}. \end{aligned} \quad (1)$$

The sensitivity of I_5 to the sign of the shear stresses is suppressed if a 'main axes transformation' around the σ_1 -axis is performed (see Figure1), leading to $\tau_{23} = 0$.

• **Strengths (Cuntze's view)**

The characterisation of the strength of transversally-isotropic composites requires –according to the FMC- the measurement of five independent basic strengths: R_{\parallel}^t , R_{\parallel}^c (fibre parallel tensile and compressive strength) as well as R_{\perp}^t , R_{\perp}^c (tensile, compressive strength transversal to the fibre direction) and $R_{\perp\parallel}$ (fibre parallel shear strength).

R_{\parallel}^t is determined by the strength of the constituent fibre and R_{\parallel}^c by 'shear instability'. The latter includes different microfailure mechanisms: The matrix may shear under loading and does not stabilise the generally somewhat misaligned fibres embedded within. Hence it comes to bending and 'kinking'⁴¹ (*structural* behaviour). Also, the load grasping fibre as stiffer constituent may shear (this is a constituent's *material* behaviour) under σ_{\parallel}^c and $\tau_{\perp\parallel}$. The strength R_{\perp}^t is determined by the relatively low strength properties of the matrix (cohesive failure), by the interphase material in the interface fibre-matrix (adhesive failure caused by a weak fibre-matrix bond), as well as by the fibres acting as embedded stress raisers.

• **Rounding-off in the Interaction Zones:**

Of further interest is the rounding-off of the fracture curve in the mixed failure domain (MiFD) or interaction or transition zone of adjacent failure modes in the envisaged lamina. In (Cun97)²⁴ a simple probabilistics-based formula -the 'Series Spring Model'- as *engineering approach* for the resultant reserve factor (which is needed anyway for the *proof of design*)

$$1/f_{\text{Res}}^{(\text{res})} = 1/f_{\text{Res}}^{\text{model1}} + 1/f_{\text{Res}}^{\text{mode2}} + 1/f_{\text{Res}}^{\text{mode3}} + \dots + \quad (2)$$

was proposed which approximates the results of a time-consuming probabilistic calculation on the safe side. In the case of residual stresses and nonlinearity instead of ~~the~~ a stress-based reserve factor $f_{\text{Res}}/f_{\text{Res}}$ the stress effort Eff has to be employed.

• **Classical Laminate Theory (CLT):**

(The CLT is addressed here mainly for the reason to depict the definitions and symbols in the German guideline VDI 2014 on 'Development of FRP components'. Sheet 3: Analysis (issued 2001) chosen after many discussions, and which will be employed here. Another reason is given by chapter 4.2)

Assuming transversal isotropy and the state of plane stress ('in-plane stressing', $\sigma_3 = 0$, which is the situation of the case studies investigated) the linear stress-strain relations for the k'th lamina of a multilayered laminate are (using matrix notation; $1 = \parallel$, $2 = \perp$, $12 = \perp\parallel$; $[Q]$, $[S]$: = stiffness, compliance matrix of the lamina)

$$\{\varepsilon\}_k = (\varepsilon_1, \varepsilon_2, \gamma_{12})_k^T = [S]_k \{\sigma\}_k \quad \text{and} \quad (3a)$$

$$\{\sigma\}_k = (\sigma_1, \sigma_2, \tau_{12})_k^T = [Q]_k \{\varepsilon\}_k. \quad (3b)$$

The symmetric *elasticity matrix of stiffness* (stiffness matrix) of the lamina reads:

$$[Q]_k = \begin{bmatrix} Q_{11} & Q_{12} & Q_{16} \\ Q_{21} & Q_{22} & Q_{26} \\ Q_{61} & Q_{62} & Q_{66} \end{bmatrix}_k = \begin{bmatrix} \frac{E_{\parallel}}{1-\nu_{\parallel\perp}\nu_{\perp\parallel}} & \frac{\nu_{\perp\parallel}E_{\parallel}}{1-\nu_{\parallel\perp}\nu_{\perp\parallel}} & 0 \\ \frac{\nu_{\perp\parallel}E_{\perp}}{1-\nu_{\parallel\perp}\nu_{\perp\parallel}} & \frac{E_{\perp}}{1-\nu_{\parallel\perp}\nu_{\perp\parallel}} & 0 \\ 0 & 0 & G_{\parallel\perp} \end{bmatrix}_k, \quad (4)$$

$$\text{with } [Q]_k^{-1} = [S]_k, \quad \nu_{\perp\parallel} \cdot E_{\perp} = \nu_{\parallel\perp} \cdot E_{\parallel} \quad (5)$$

and $\nu_{\perp\parallel}$ as the *major* Poisson's ratio (Maxwell-Betti)! Thus, for the application of CLT the knowledge of only four constants is essential: E_{\parallel} , E_{\perp} , $G_{\parallel\perp}$ and $\nu_{\perp\parallel}$ ($\equiv \nu_{12}$ in 'failure exercise'³).

In the case of mechanical loading

the following load-strain equations are obtained in the cross section for the load fluxes $\{n\}$ and the moment fluxes $\{m^{\circ}\}$ (moment per width)

$$\begin{Bmatrix} n \\ m^{\circ} \end{Bmatrix} = \begin{bmatrix} A & B \\ B & D \end{bmatrix} \begin{Bmatrix} \varepsilon^{\circ} \\ \chi \end{Bmatrix} = [K] \begin{Bmatrix} \varepsilon^{\circ} \\ \chi \end{Bmatrix} \quad (6)$$

with $[K]$ being the *stiffness matrix of the laminate*, from which will be utilized the extensional stiffness matrix (see 'Theory of Laminated Plates' by Ashton/Whitney)

$$[A] = \sum_{k=1}^n [Q']_k \cdot t_k, [Q'] = [T_{\sigma}] [Q] [T_{\sigma}]^T, \quad (7)$$

and transformation matrices ($s = \sin \alpha$, $c = \cos \alpha$)

$$[T_{\sigma}] = \begin{bmatrix} c^2 & s^2 & -2sc \\ s^2 & c^2 & 2sc \\ sc & -sc & c^2 - s^2 \end{bmatrix}, [T_{\varepsilon}] = \begin{bmatrix} c^2 & s^2 & -sc \\ s^2 & c^2 & sc \\ 2sc & -2sc & c^2 - s^2 \end{bmatrix}. \quad (8a, b)$$

Having determined the strain vector $\{\varepsilon^{\circ}\}$ and the curvature vector $\{\chi\}$ for the middle plane of the laminate, the so-called natural strains $\{\varepsilon\}_k$ (strains in the lamina coordinate system) and stresses $\{\sigma\}_k$ in each lamina may be calculated according to

$$\{\varepsilon\}_k = [T_{\sigma}]_k^{-1} (\{\varepsilon^{\circ}\} + z\{\chi\}), \quad (9a, b)$$

$$\{\sigma\}_k = [Q]_k \{\varepsilon\}_k.$$

The equations above decouple for a symmetric lay-up to

$$\{\varepsilon^{\circ}\} = [A]^{-1} \{n\}. \quad (10)$$

If curing stresses have to be considered the equations read

$$\{\varepsilon^{\circ}\} = [A]^{-1} (\{n\} + \{n_T\}) \quad \text{with} \quad (11)$$

$$\{n_T\} = \sum_{k=1}^n \Delta T [Q']_k t_k \{\alpha'_T\}_k \quad \text{and} \quad (12)$$

$$\{\alpha'_T\}_k = [T_{\varepsilon}]_k \{\alpha_T\}_k, \quad \{\alpha_T\} = (\alpha_{T\parallel}, \alpha_{T\perp}, 0)^T. \quad (13a, b)$$

In the case of symmetrical lay-ups (test cases of the 'failure exercise'), for the treatment of *material nonlinearity* and of *degradation*, the lamina stresses $\{\sigma\}_k$ have to be computed considering

$$\{\varepsilon'\}_k = \{\varepsilon^{\circ}\} \quad \dots \quad \text{compatibility} \quad (14)$$

$$\{\sigma'\}_k = [Q']_k \cdot (\{\varepsilon'\}_k - \{\varepsilon'_T\}_k) \quad \dots \quad \text{Hooke} \quad (15)$$

$$\{\sigma\}_k = [T_{\sigma}]_k^{-1} \cdot \{\sigma'\}_k, \quad \{\varepsilon\}_k = [T_{\varepsilon}]_k^{-1} \{\varepsilon'\}_k \quad (16)$$

and applying

$$[\mathbf{T}_\sigma]^{-1} = [\mathbf{T}_\varepsilon]^T, [\mathbf{T}_\varepsilon]^{-1} = [\mathbf{T}_\sigma]^T. \quad (17a, b)$$

The definitions for the lamina (often called ply if it is a prepreg and layer if it is winding) stresses, angles and thicknesses are illustrated in Figure 2.

The index k of the single lamina will be dropped in the further text.

4 FAILURE MODES AND FAILURE CONDITIONS OF A LAMINA

Failure conditions⁴⁹⁻⁵⁷ should exhibit –besides a sound physical basis– the numerical advantages: mathematical homogeneity (see F_\perp^τ in Annex 4 after the homogenization) in the stress terms, stress terms of the lowest degree, simplicity, scalar formulations and therefore invariant, numerical robustness and rapid computation.

4.1 Failure modes (types)

A designer has to dimension a laminate versus inter-fibre-failure (IFF) and fibre-failure (FF). IFF normally indicates the *onset of failure* whereas the appearance of FF in a single lamina of the laminate usually marks *final failure*. In the case of brittle behaving FRP, the failure is a fracture. The IFF incorporates cohesive fracture of the matrix and adhesive fracture of the fibre-matrix interface.

Fracture is understood in this article as a separation of material, which was free of damage such as technical cracks and delaminations but not free of tiny defects/flaws (size of microns) prior to loading.

Figure 3 informs about the *types of fracture* which are recognised in case of 'dense' (means: 'not porous') transversally-isotropic *ideal materials*.

Whether a failure may be called a shear stress induced shear failure, SF, or a normal stress induced normal failure, NF, depends on the size scale applied. $SF_{\perp\parallel}$ shows macroscopically shear failure (fracture plane is parallel to τ_{21}). However micromechanically, it is a 45° normal failure mode of the matrix, caused by tensile matrix stress and visualised by the so-called hackles⁴¹. These microcracks grow until they touch the next fibre layer where they are turned to later form the basis for the fibre-parallel IFF.

The 'explosive' effect of a so-called *wedge shape* failure (a σ_\perp^c -caused IFF) of an embedded lamina of the laminate may directly lead⁴² to final failure (see a torsion spring) or via local delaminations to buckling of the adjacent laminae and therefore to final failure, too. This IFF, may also cause a catastrophic failure like FF.-

4.2 Strain energy density basis

Beltrami, Schleicher et al. assume at initiation of yield that the strain energy density will consist of two portions. Thus, the strain energy (denoted by W) in a cubic element of a material reads

$$W = \int \{\sigma\} \{\varepsilon\} d\{\varepsilon\} = W_{\text{Vol}} + W_{\text{shape}}. \quad (18)$$

Including Hooke's law in the case of a transversally-isotropic body the expression will take the shape (see Lechnitski, s_{ik} = compliance coefficients analogue to the 2D formulation of eqn (3a). See also (Ashton/Whitney)):

$$\begin{aligned} W &= [s_{11} \sigma_1^2 + s_{22} \sigma_2^2 + s_{33} \sigma_3^2 + s_{44} \tau_{23}^2 + \\ &\quad + s_{55}(\tau_{12}^2 + \tau_{13}^2)]/2 + s_{12} (\sigma_1 \sigma_2 + \sigma_1 \sigma_3) + \\ &\quad + s_{23} \sigma_2 \sigma_3 \\ &= \frac{I_1^2}{2E_\parallel} + \frac{I_2^2(1-\nu_{\perp\perp})}{4E_\perp} - \frac{\nu_{\perp\parallel} I_1 I_2}{E_\parallel} + \frac{I_3}{2G_{\perp\perp}} + \frac{I_4(1+\nu_{\perp\perp})}{4E_\perp}. \end{aligned} \quad (19)$$

volume volume volume shape shape

Some of the terms above describe the *volume* change of the cubic material element and others its change of the *shape*. These changes can be witnessed by the fracture morphology⁴¹.

In order to formulate a relatively simple failure condition one chooses as basic invariant that term in eqn(19) which respects whether the cubic material element will experience a volume change in the considered mode or a shape change.

4.3 Failure conditions achieved

In engineering application due to property scatter the simplest strength criteria which still describe the physical effects should be applied. This always reduces the number of curve parameters (inherent in the failure criteria) to be determined and, besides this, the numerical effort. Applying the FMC in total three (statistically-based) calibration points at maximum have to be experimentally determined besides the basic strengths serving as anchor points in each mode failure domain.

Based on the idea above the following *failure conditions*, $F(\{\sigma\}) = 1$ have been derived

$$\begin{aligned}
 \text{FF1: } F_{\parallel}^{\sigma} &= \frac{I_1^*}{\bar{R}_{\parallel}^t} = 1, & \dots\dots \text{FF} & (20) \\
 \text{FF2: } F_{\parallel}^{\tau} &= \frac{-I_1}{\bar{R}_{\parallel}^c} = 1, \\
 \text{IFF1: } F_{\perp}^{\sigma} &= \frac{I_2 + \sqrt{I_4}}{2\bar{R}_{\perp}^t} = 1 & \dots\dots \text{IFF} & \\
 \text{IFF2: } F_{\perp\parallel} &= \frac{I_3^{3/2}}{\bar{R}_{\perp\parallel}^3} + b_{\perp\parallel} \frac{I_2 I_3 - I_5}{\bar{R}_{\perp\parallel}^3} = 1, \\
 \text{IFF3: } F_{\perp}^{\tau} &= (b_{\perp}^{\tau} - 1) \frac{I_2}{\bar{R}_{\perp}^c} + \frac{b_{\perp}^{\tau} I_4 + b_{\perp\parallel}^{\tau} I_3}{\bar{R}_{\perp}^{c2}} = 1
 \end{aligned}$$

with three free curve parameters ($b_{\perp\parallel}, b_{\perp}^{\tau}, b_{\perp\parallel}^{\tau}$) to be determined from multiaxial test data: (\bar{R} marks mean strength value. * Mind: $\sigma_1 \rightarrow v_f \cdot \sigma_{1f} = v_f \cdot \varepsilon_1 \cdot E_{1f} = \varepsilon_1 \cdot E_{\parallel}^t$ with σ_{1f} = tensile stress fibre and $v_f :=$ fibre volume fraction. The very small load-carrying capacity of the matrix is neglected here in relation to the fibre's. $F=1$ is called criterion)

. Each of them has to be calculated from a test point (several measurements) or by curve fitting of the course of test data in the associated pure domain. The (calibration points in the Figures 4,5 deliver, after inserting them into the equations IFF2, 3 and a further resolution, the equations

$$b_{\perp\parallel} = \frac{1 - \left(\tau_{21}^{\perp\parallel} / \bar{R}_{\perp\parallel}\right)^2}{2\sigma_2^c \cdot \tau_{21}^{\perp\parallel 2} / \bar{R}_{\perp\parallel}^3} \quad \text{from } \left(\sigma_2^c, \tau_{21}^{\perp\parallel}\right) \quad (21a)$$

$$b_{\perp}^{\tau} = \frac{1 + (\sigma_2^{c\tau} + \sigma_3^{c\tau}) / \bar{R}_{\perp}^c}{(\sigma_2^{c\tau} + \sigma_3^{c\tau}) / \bar{R}_{\perp}^c + (\sigma_2^{c\tau} - \sigma_3^{c\tau})^2 / \bar{R}_{\perp}^{c2}} \quad \square \quad (21b)$$

$$b_{\perp\parallel}^{\tau} = 1 - (b_{\perp}^{\tau} - 1) \sigma_{2\perp\parallel}^{c\tau} / \bar{R}_{\perp\parallel} - b_{\perp}^{\tau} (\sigma_{2\perp\parallel}^{c\tau} / \bar{R}_{\perp\parallel})^2 \quad (21c)$$

for the parameter determination. The parameters depend on the material behaviour and on the IFF formulation applied. Bounds on the safe side for GFRP, CFRP and AFRP are assumed to be

$$0.05 < b_{\perp\parallel} < 0.15, \quad 1.0 < b_{\perp}^{\tau} < 1.6, \quad 0 < b_{\perp\parallel}^{\tau} < 0.4 .$$

The extreme value $b_{\perp\parallel} = 0$ means 'no bulge effect' and $b_{\perp}^{\tau} = 1$ means 'no friction' in the $\perp\perp$ -plane. Above bounds for the parameters and later the mapping of the failure curves are based on multiaxial test data cited in literature⁵⁻⁷ or carried out at MAN⁺.

The author's practice shows: Often, $b_{\perp\parallel}^{\tau} = 0$ will map the lamina test data well enough. The skill has to be put into m as a rounding coefficient on the safe side. Data for the computation of $b_{\perp\parallel}$ (Fig.4) are numerous, $b_{\perp\parallel} = 0.1$ is a good approach. As calibration points for b_{\perp}^{τ} are still missing in the quasi-isotropic domain knowledge from brittle isotropic material is applied which will keep the engineer in the compression domain on the safe side by assuming $b_{\perp}^{\tau} = 1$.

In the following text the reasons are depicted for the application of Which invariant? and of Which form of invariant? (success check was the mapping of the available multiaxial data):

- F_{\parallel}^{σ} : According to the FMC, F_{\parallel}^{σ} originally consists of a quadratic term in stresses. However, being the only (basic) term, the quadratic term can be replaced by a numerically simpler linear term which regards that the fibre tensile stress and not σ_1 (the UD 'material' model does not hold here) has to be applied if formulating a failure condition. Eqn(20a) indicates that for FF not σ_1^t has to reach the value for the UD-strength R_{\parallel}^t but $\varepsilon_{\parallel} \cdot E_{\parallel}$. Why? Poisson's effect is not negligible, because a compressive lamina stress state (σ_2^c, σ_3^c) will cause tensile fibre stress. $FF^{\sigma} = 1$ theoretically may be reached without a load stress σ_1^t !

- F_{\parallel}^{τ} : Again the basic term is I_1^2 . For reasons of simplicity and due to lacking of test data in the (σ_2^c, σ_3^c) domain, a shear addressing invariant I_3 (reflecting some W_{shape}) was not considered in F_{\parallel}^{τ} . By this, the I_1^2 could be reduced to the linear basic term I_1 .

- $F_{\perp\parallel}$: Basic term is I_3 . The choice of the failure condition is strongly affected by the 'easy to be used' ~~wish~~-desire and by an easy determination of f_{Res} , which is simplified if $F(\{\sigma\})$ is a so-called homogeneous function wherein the stress terms are of the same power (grade). Therefore $I_3^{3/2} / \bar{R}_{\perp\parallel}^3$ was applied, instead of a quadratic formulation which was used in the past, thus leading to homogeneity of $F_{\perp\parallel}$. The term $I_2 I_3 - I_5$ is the result of an intensive analytical 'trial and error search' of the first author. It respects the different interaction of the stress combinations (σ_2, τ_{21}) and (σ_2, τ_{31}) a typical material asymmetry at first described by Puck and proven by test⁶ (not considerable by Tsai/Wu).

A numerical problem existing in $F_{\perp\parallel}$ has to be mentioned: If $b_{\perp\parallel}$ ($I_2 I_3 - I_5$) becomes $I_3^{3/2}$, then the $\tau_{21}(\sigma_2)$ -curve in Fig.4 turns to infinity. In order to generally bypass this difficulty one has to ~~question this~~ put a query in the program and replace, if applicable, the formulation of the off-turning $F_{\perp\parallel}$ curve by a limiting 'horizontal' line defined by the constant $\max I_3^{3/2}$ (see Annex A4)-value. This is very simply done for the 2D test cases. ~~Ideas how this problem may be generally solved are presented in Annex 4.~~

- F_{\perp}^{σ} : After another intensive search the really straight line in the quasi-isotropic (σ_2, σ_3) -plane could be mapped by employing $I_2 + \sqrt{I_4}$ in F_{\perp}^{σ} (I_2 is the section line with a hyperbola. Known from isotropy).

- F_{\perp}^{τ} : In F_{\perp}^{τ} , besides the basic term I_4 , the linear term I_2 was applied which considers friction. If really necessary, a term I_3 may additionally be taken aiming at a better numerical rounding-off in the $(F_{\perp}^{\tau}, F_{\perp\parallel})$ -interaction zone.

On the other hand, if I_3 is not applied that means sticking to the basic FMC ($b_{\perp\parallel}^{\tau}=0$), F_{\perp}^{τ} ~~may~~ can be homogenized, too, by replacing I_4/R_{\perp}^{c2} by $\sqrt{I_4}/R_{\perp}^c$. This will lead from a parabola (~~still almost straight in fig. 5~~) (is in the negative domain already almost straight in Fig. 5 for the parabolic formulation) to a straight line for $\sigma_2^c(\sigma_3^c)$, and shall be the authors' engineering choice in future (see Annex 4).

-

With respect to the 3D character of the IFF conditions above they may serve also as criteria for the *onset of delamination* (F_{\perp}^{τ} : wedge failure, F_{\perp}^{σ} : transversal tensile failure) generated by the interlaminar stresses $\sigma_3, \tau_{32}, \tau_{31}$. Hydrostatic compressive and tensile stressing is automatically considered.

One has to keep in mind: One or two modes will be the design driving ones in a local 'material' point of a composite's lamina. The basic strength of the mode-related linear or nonlinear stress-strain curve controls the (size) *volume* of the mode failure surface (body) being one part of the global failure surface (body). Curve parameters are representing an effect, such as friction (b_{\perp}^{τ}) in the material. They control the *shape* of the mode failure surface.

5 RESERVE FACTORS $f_{Res}^{(mode)}$, $f_{Res}^{(res)}$ OF THE LAMINA

5.1 General

Reserve factors which have to be determined for the *Proof of Design* of each lamina in the laminate are defined *load-related*. These are:

- for the *initial failure*, indicated by the so-called knee in the laminate's stress-strain curve and originated by F_{\perp}^{σ} , $F_{\perp\parallel}$ in the laminae

$$f_{Res}^{initial} = \frac{\text{initial failure load}}{j_{p0.2} \cdot DLL}, \text{ and} \quad (22a)$$

- for the *final failure*, indicated by F_{\parallel}^{σ} , F_{\parallel}^{τ} or F_{\perp}^{τ} ,

$$f_{Res}^{final} = \frac{\text{final failure load}}{j_{ult} \cdot DLL} \quad (22b)$$

with $DLL :=$ Design Limit Load and

$j_{p0.2}, j_{ult} :=$ design factors of safety (FoS).

The various failure loads to be inserted into the eqns(22) are either a result from experiment or from analysis(applying a failure criterion).

In *linear* analysis the reserve factor f_{Res} is normally defined that factor all *mechanical load-induced* stresses applied to the laminae have to be multiplied with in other to generate failure. Geometrically it means that the stress vector $\{\sigma\}_{(L)}$ has to be stretched in its original direction by this factor in order to cause failure. This visualisation is valid as far as *linear* modelling can be applied: If there are no residual stresses and high design *factors of safety* (FoS), j , then a linear elastic modelling is permissible and a *stress-based* f_{Res} can be predicted.

In case of *nonlinear* behaviour accurate reserve factors have to be referred to loads, which is in accordance to the fact that *load* FoS are given. Analysis provides via the failure criterion

with the modes' *equivalent stresses* σ_{eq} and *stress efforts* E_{eff} outlining the remaining load capacity for the computation of the resultant reserve factor. The value of the reserve factor then is the ratio

$$f_{Res} = \frac{\text{failure load at } Eff^{(res)} = 1}{j \cdot DLL} .$$

As failure load often taken is the maximum load achieved when computation stops due to numerical problems. Nonlinear analysis in general means stress redistribution in the *structure*. This lowers the stress level of the 'hot spots' in the laminae (defined *material*) of the laminate.

5.2 Determination of Mode reserve factors

If linear analysis is permitted:

- Case "No residual stresses": $\{\sigma\}_{(L)} = f(j \cdot DLL)$

$$\{\sigma\}_{failure} = f_{Res} \cdot \{\sigma\}_{(L)} = \{\sigma\}_{(L)} + MS \cdot \{\sigma\}_{(L)} \quad (23)$$

with the margin of safety $MS = f_{Res} - 1$.

Inserting above definition into the failure condition

$$F = F(\{\sigma\}_{Failure}) = F(f_{Res} \cdot \{\sigma\}_{(L)}) = 1$$

yields an equation for the *stress-based* f_{Res}

$$f_{Res} \cdot \ell_{(L)} + f_{Res}^2 \cdot q_{(L)} + f_{Res}^3 \cdot c_{(L)} + \dots = 1.$$

* Special example: The failure condition only has linear and quadratic stress terms.

Then the reserve factor can be calculated (Cun96)²³ by resolving for f_{Res} as of a polynomial a root which delivers (mind: $\bar{R} \rightarrow R!$ in the case of *Proof of Design*)

$$f_{Res} = 1/\ell_{(L)} \quad (\text{e.g. } = 1/(v_f \cdot I_{1f}/R_{\parallel}^t)) \quad \dots \text{ linear} \quad (24a)$$

$$f_{Res} = \left(-\ell_{(L)} + \sqrt{\ell_{(L)}^2 + 4q_{(L)}} \right) / 2q_{(L)} \quad \dots \text{quadr.} \quad (24b)$$

with $\ell_{(L)} = \Sigma$ linear terms, $q_{(L)} = \Sigma$ quadr. terms.

- Case "With residual stresses" (linear modelling)

$$\{\sigma\}_{failure} = f_{Res} \cdot \{\sigma\}_{(L)} + \{\sigma\}_{(R)} . \quad (25)$$

In the case of linear terms, after substitution of the failure causing state of stress one yields

$$F = F(\{\sigma\}_{Failure}) = F(f_{Res} \cdot \{\sigma\}_{(L)} + \{\sigma\}_{(R)}) = 1 \quad (26)$$

with $\{\sigma\}_{(R)}$ from curing stresses' computation etc. This procedure can be applied as long as the residual stresses have not caused an essential amount of damage which would lead to stress-redistribution and a reduction of the size of the residual stresses.

5.3 Determination of resultant reserve factor (rounding-off of failure modes)

The (*resultant*) *Reserve Factor* (superscript res) takes account of the interactions of all modes. In case of *linearity* it may be estimated (Figure 4 just includes the relevant interacting modes) by the rounding-off equation or *spring model*

$$\begin{aligned} (1/f_{Res}^{(res)})^{\dot{m}} &= f(f_{Res}^{(modes)}) \\ &= (1/f_{Res}^{\perp\sigma})^{\dot{m}} + (1/f_{Res}^{\perp\parallel})^{\dot{m}} + (1/f_{Res}^{\perp\tau})^{\dot{m}} + (1/f_{Res}^{\parallel\sigma})^{\dot{m}} + (1/f_{Res}^{\parallel\tau})^{\dot{m}} \end{aligned} \quad (27)$$

with \dot{m} as the rounding-off *coefficient* exponent. As a simplifying *assumption*: \dot{m} is taken the same for each interaction zone. The value of \dot{m} has to be set by fitting experience and by respecting the fact that in the interaction zones micromechanical and probabilistic effects will commonly occur and cannot be discriminated. From numerical *experience*—reasons \dot{m} *is* should be an odd number between 3 and 4.

If inserting a unidirectional fracture stress (this is the strength value) into the equation above, then a failure curve or a failure surface described by $f_{Res}^{(res)} = 1$ is achieved.

Figure 5 refers to the (σ_2, σ_3) -plane as one failure plane of the various ones. In the upper part it visualizes the evaluation of test data and in the bottom part the rounding-off (by the spring model) in the multifold (MfFD) and mixed failure domains (MiFD) as well as the shrunk design space (mean strength \bar{R} of mapping is replaced by a *strength design allowable* R) to be used by the designer in the 'dimensioning' and in the 'proof of design'. The rounding shown in the Figures 4 and 5 *seems* to exclude the FF modes. These modes, however, have no relevant interaction with the failure curves $\tau_{21}(\sigma_2)$ and $\sigma_2(\sigma_3)$.

Additionally to the FMC-based 'Mode Fit' the 'Global Fit' (e.g. Tsai/-Wu's 'single failure surface' criterion describes a global failure surface or body) is pointed out. The Global Fit interacts between the UD-stresses *and* the *independent* failure modes in one equation, achieving a description of the global (complete) failure surface. This procedure is simple, however error-prone in some domains, due to its physical shortcomings.

In order to consider failure probability or the multifold failure chances in the (σ_2^t, σ_3^t) -domain (MfFD) the term $(1/f_{Res}^{\perp\sigma})^m$ has to be made 'twofold' effective. A simple numerical way to implement this is by including in eqn(27) **and will be replaced by** (see Figure 5),

via $(1/f_{Res}^{\perp\sigma})^m + (1/f_{\perp}^{MfFD})^m$,

the multifold failure term (~~Awa78~~)⁴³.

$$f_{\perp}^{MfFD} = 2R_{\perp}^t / (\sigma_2^t + \sigma_3^t) \quad . \quad (28)$$

Eqn(28) is applied only, if test data mapping makes it necessary. The experimental behaviour of brittle isotropic materials justifies the MfFD rounding in the quasi-isotropic plane of the UD-lamina.

In the following set of formula the so-called *equivalent stress* of each mode is applied. This stress includes all load stresses and residual stresses which are acting together in a mode equation.

5.4 Application to the UD-lamina (3D-conditions)

The *Mode Reserve Factors* explicitly read

$$\text{generally } f_{Res}^{(mode)} = R^{mode} / \sigma_{eq}^{(mode)}, \quad (29)$$

$$\bullet f_{Res}^{\parallel\sigma} \hat{=} R_{\parallel}^t / (\varepsilon_1 \cdot E_{\parallel}^t) = R_{\parallel}^t / \sigma_{eq}^{\parallel\sigma}, \quad (30a)$$

$$\bullet f_{Res}^{\parallel\tau} = -R_{\parallel}^c / \sigma_1 = -R_{\parallel}^c / \sigma_{eq}^{\parallel\tau}; \quad (30b)$$

$$\bullet f_{Res}^{\perp\sigma} = \frac{2R_{\perp}^t}{I_2 + \sqrt{I_4}} = \frac{R_{\perp}^t}{\sigma_{eq}^{\perp\sigma}}, \quad (30c)$$

$$\bullet f_{Res}^{\perp\tau} = \frac{R_{\perp}^c}{2} \cdot \frac{(-b_{\perp}^{\tau} - 1)I_2 + \sqrt{(b_{\perp}^{\tau} - 1)^2 I_2^2 + 4b_{\perp}^{\tau} I_4 + 4b_{\perp\parallel}^{\tau} I_3}}{b_{\perp}^{\tau} I_4 + b_{\perp\parallel}^{\tau} I_3}, \quad (30d)$$

$$\bullet f_{Res}^{\perp\parallel} = R_{\perp\parallel} / (I_3^{3/2} + b_{\perp\parallel} (I_2 I_3 - I_5))^{1/3}. \quad (30e)$$

Remark: If a $f_{Res}^{(mode)}$ becomes negative, caused by the numerically advantageous automatical insertion of $\{\sigma\} = (\sigma_1, \sigma_2, \sigma_3, \tau_{23}, \tau_{13}, \tau_{12})^T$ as FEM output into the eqn(30), a value of +100 shall replace the negative value. A negative value eg results if a positive σ_1 (better $\varepsilon_1^t E_{\parallel}$) is inserted into eqn(30b).

For an effective design the stress engineer is provided with a table which indicates the *design driving* mode reserve factors (an example: see Annex 3).

6 EQUIVALENT STRESS, MODE EFFORT AND EFFECTIVE SECANT MODULI

In the case of small FoS (eg in spacecraft) just *nonlinear* analyses will enable the stress engineer to predict the stress effort and then the load-based f_{Res} . The actual stress effort of a mode, $Eff^{(mode)}$, is the actual portion of the maximum 100 % achieved at mode failure. The procedure of determining the resultant stress effort $Eff^{(res)}$ in each lamina of the laminate is similar to that of $f_{Res}^{(res)}$. The stress effort (Puck calls it stress exposure factor f_E) can be related to the reserve factor in case of *linear* behaviour and zero residual stresses, that means on stress level, by

$$Eff^{(res)} = 1 / f_{Res}^{(res)} . \quad (31)$$

Also similar to the ' $f_{Res}^{(res)}$ procedure' at first the *equivalent stress* vector

$$\left\{ \sigma_{equiv}^{(modes)} \right\} = \left(\sigma_{eq}^{\parallel\sigma}, \sigma_{eq}^{\parallel\tau}, \sigma_{eq}^{\perp\sigma}, \sigma_{eq}^{\perp\tau}, \sigma_{eq}^{\perp\parallel} \right)^T \quad (32)$$

will be computed. It includes the equivalent stress of each mode of the lamina and within the nonlinearly load dependent load stresses $\{\sigma\}_{(L)}$ and the equally nonlinearity-dependent residual stresses $\{\sigma\}_{(R)}$ from curing etc.

Consequently the *resultant stress effort* is represented by

$$\begin{aligned} Eff^{(res)m} &= \sum_1^5 Eff^{(modes)} \\ \text{---} &= \left(\sigma_{eq}^{\parallel\sigma} / \bar{R}_{\parallel}^t \right)^m + \left(\sigma_{eq}^{\parallel\tau} / \bar{R}_{\parallel}^c \right)^m + \left(\sigma_{eq}^{\perp\sigma} / \bar{R}_{\perp}^t \right)^m + \\ &+ \left(\sigma_{eq}^{\perp\tau} / \bar{R}_{\perp}^c \right)^m + \left(\sigma_{eq}^{\perp\parallel} / \bar{R}_{\perp\parallel} \right)^m . \end{aligned} \quad (33)$$

with $Eff^{(modes)}$ corresponding to some extent to the $f_E^{(domains)}$ of Puck (see Annex 1).

In case of fracture stresses holds, analogous to $f_{Res}^{(res)} = 1$,

$$Eff^{(res)} = 1 = 100\% . \quad (34)$$

Usually in the laminae of a laminate, multiaxial states of stress are acting which have an impact on more than one of the failure modes. Because in the interaction domains adjacent failure modes are commonly affected, a corresponding degradation (displayed by a stiffness reduction) has to be considered by a drop in the secant moduli applied in the nonlinear analysis. A 'triggering' of the adjacent equivalent stresses takes into account this effect for each of the associated moduli. As 'triggering approach' is recommended (see also Annex A1.2):

- for *increasing* stress (*Hardening*) $\Delta\sigma > 0$

$$\text{corr-} \sigma_{eq}^{>(mode)} = \sigma_{eq}^{(mode)}$$

being an ~~influence~~ modulus ~~decrease~~ (35a)

- for *decreasing* stress (*Softening*) $\Delta\sigma < 0$

$$\text{corr-} \sigma_{eq}^{<(mode)} = \sigma_{eq}^{(mode)} / TrF$$

being an ~~influence~~ modulus decrease, (35b)

with the triggerfactor $TrF = Eff^{(res)} / \max Eff^{(mode)}$. (36)

In these equations the stress effort of the maximum stressed mode governs the 'triggering' and TrF is dedicated to all IFF modes affected. As eqn(36) leads to a sharp decay, a damped

triggering according to $\text{newTrF} = \sqrt[n]{\text{TrF}}$ is proposed for the future.

This approach has to be verified -before general acceptance- for all possible stress combinations ~~possible~~, of course (see also Annex A1.2).

7 DESCRIPTION OF NON-LINEARITY

Nonlinear behaviour⁵⁸⁻⁶⁰ of well-designed composites is most often physically (laminae behaviour) but rarely geometrically (laminated behaviour) caused.

A full 3D-input in *stress analysis* demands for 5 elastic properties in the case of Fibre Reinforced Plastics (FRP) and in *strength analysis* for 5 strengths. In the 2D-case the required input consists in 4 elastic properties and 5 strength properties.

Further, for the nonlinear stress analysis ~~additionally~~ the relevant nonlinear stress-strain curves are to be provided, which should discriminate the so-called hardening and the softening (Figure 7-6). Material *hardening* is the domain until the stress reaches its strength value R_m which addresses here an initial failure level of IFF type. From that level on, that means for the *progressive failure* or damage regime, the term *softening* is used. Of course, some damaging already begins with material hardening.

7.1 Mapping of hardening

The degree of nonlinearity essentially depends on the nonlinearly behaving matrix material which affects E_{\perp}^c and $G_{\parallel\perp}$. For the secant moduli to be applied in the nonlinear stress analysis the following values are determined by the Ramberg/Osgood equation which maps the course of nonlinear stress-strain data very well (with $E_{(o)}$ the initial tangent modulus)

$$\varepsilon = \sigma / E_{(o)} + 0.002(\sigma / R_{p0.2})^n \quad (37)$$

with the Ramberg/Osgood exponent (see Mil Hdbk 5)

$$n = \ln(\varepsilon_{pl}(R_m)) / \ln(R_m / R_{p0.2}) \quad (38)$$

estimated from the strength point $(R_m, \varepsilon_{pl}(R_m))$. Data for the secant moduli of E_{\perp} , $G_{\parallel\perp}$ are provided from above Ramberg/Osgood mapping of test data course (denotations see Figure 6) by

$$E_{(sec)} = E_{(o)} / (1 + 0.002 \cdot E_{(o)} / R_{p0.2} \cdot (\sigma / R_{p0.2})^{n-1}) \quad (39)$$

7.2 Mapping of softening

Above the *Initial Failure* level an appropriate progressive failure analysis method has to be employed (or a *Successive Degradation Model* for the description of *post initial* failure) by using a failure mode condition that indicates failure type and damage danger (level of stress effort). *Final Failure* occurs after the laminate (and thereby the structure) has experienced a stiffness reduction and has degraded to a level where it is no longer capable of carrying additional load.

Figure 6 depicts hardening with softening. In detail: (a) for an *isolated* eg tensile coupon specimen in the usual load controlled test, (b) in a strain controlled test. A measurement of curve (b) would be possible at the institute BAM in Berlin, which possesses a test rig of a very high frame stiffness, however, tests have not yet performed. The curve (b) is assumed here due to the lack of experimental data from there.

Modelling of *Post Initial Failure* behaviour of a laminate requires that assumptions have to be made regarding the decaying elastic properties of the actually degrading embedded lamina (curve (c) in Figure 7). E_{\perp}^c and $G_{\parallel\perp}$ are decreasing gradually rather than being suddenly annihilated. A ~~rapid~~ rapid collapse (often named 'ply discount method') of E_{\perp}^t is unrealistic and ~~further~~ probably further leads to convergence problems.

A simple function was used to map this softening, in order to later derive the secant moduli. It generally reads (the suffix *s* denotes softening)

$$\sigma_s = R_m / (1 + \exp[(a_s + \varepsilon) / b_s]) \quad (40)$$

with two curve parameters a_s , b_s to be estimated by the data of two calibration points, e.g.

$$(R_m, \varepsilon(R_m)) \text{ and } (R_m \cdot 0.5, \varepsilon(R_m \cdot 0.5)). \quad (41)$$

Above softening function (eqn(40)) practically models the stress-strain curve of a lamina which is embedded in a laminate, and thus, it includes the effect of the altering microcrack density up to the critical damage state (CDS). Curve (c) is therefore an *effective* curve.

7.3 Constraint effect of on an embedded laminae

If applying test data from tensile coupons to an embedded lamina in a laminate, one has to consider that tensile coupon tests deliver test results of *weakest link type* (series model). An embedded⁴⁰ or even an only one-sided constraint lamina, however, belongs to the class of *redundant types* behaviour, to the 'parallel spring model' type. Due to being strain-controlled the material flaws in a *thin* lamina cannot grow freely up to microcrack size in thickness direction, because the neighbouring laminae will act as microcrack-stoppers (problem of energy release in fracture mechanics).

Cuntze sees the peak value of so-called *effective* stress-strain curve (in-situ, *embedded lamina*) a slightly higher than the strength point \bar{R} of the *isolated* specimen due to the change from the 'weakest link behaviour' to the real redundant behaviour (Figure 7) of a laminate.

For ~~reasons~~ the sake of simplicity this 'peak value' is lowered down to \bar{R} in the following analytical description of softening.

For the execution of nonlinear analysis the application of an *effective* stress-strain curve is necessary which estimates the behaviour of the lamina in the laminate regarding the stack, its position, and the thickness.

In order to provide the nonlinear analysis with the input needed, normalized stress-strain curves have been constructed (Figure 8) with a hardening part measured and a softening part assumed (as long as no test data are available)

In the nonlinear analysis normally mean values have to be regarded in order to perform a stress analysis that corresponds to an average *structural behaviour*. Therefore, when executing a nonlinear *stress* analysis of the structure, the secant moduli to be utilized are *mean* values, too. However later, ~~in~~ in the *strength* analysis of the 'hot spots' (*Proof of Design*) so-called 'A' or 'B' design allowables⁴⁴ as minimum strength values R have to be regarded.

For simply deriving *clear* data for the secant moduli two regimes have to be distinguished: one below and one above $\varepsilon(\bar{R}_m)$.

~~In order to provide the nonlinear analysis with the input needed normalized stress-strain curves have been constructed with a hardening part measured and a softening part assumed (Figure 8).~~

7.4 Choice of different *m* values

In the rounding-off or interaction equation just one constant value for \dot{m} is inserted. This might not work if the interaction effects covered by refined conditions (eg Cun98)²³ are replaced by more practicable simpler formulations, (eg setting $b_{\perp\parallel}^{\tau} = 0$, Annex 4). In that case the rounding-off equation may be split into several mode interaction formulae replacing the single equation, because interaction addresses two or at maximum three of the five modes, only. The advantage of this computing intensive procedure would be the possibility of accounting for different values with respect to different interaction effects in the various mode interaction domains.

If the failure curve is reached, then $f_{Res}^{(res)} = 1$, and for this level one can stay with the advantage of one single formula. Due to the fact that $1^m = 1^{x \cdot m}$ different interaction effects can be accounted for. A recommendation of the author for an improved treatment of the micromechanically linked modes F_{\perp}^{σ} and $F_{\perp\parallel}$ is derivable from

$$1 = \left(1/f_{Res}^{\parallel\sigma}\right)^{m_1} + \dots + \left(1/f_{Res}^{\perp\sigma}\right)^{m_3} + \left(1/f_{Res}^{\perp\parallel}\right)^{m_4} + \dots \quad (42)$$

Utilizing different exponents the solution has to be achieved iteratively :

$$\{\sigma\}_{(L)} \rightarrow f_{Res}^{(res1)}, \quad f_{Res}^{(res1)} \cdot \{\sigma\}_{(L)} \rightarrow f_{Res}^{(res2)},$$

$$f_{Res}^{(res2)} \cdot f_{Res}^{(res1)} \{\sigma\}_{(L)} \rightarrow f_{Res}^{(res3)} \text{ until } f_{Res}^{(resj)} \approx 1.$$

Hence will be $f_{Res}^{(res)} = f_{Res}^{(res1)} \cdot f_{Res}^{(res2)} \dots$

The procedure for the stress effort $Eff^{(res)}$ is analogous.

7.5 Variation of Poisson's ratio

The alteration of the major Poisson's ratio $\nu_{\perp\parallel}$ (notation VDI 2014) is linked to the associated failure mode. ~~E-gg-~~ in the case of shear failure under compressive lateral stresses the value for $\nu_{\perp\parallel}$ will be higher than for tensile lateral stresses. Respecting the low effect Poisson's ratios have -if using FRP with stiff fibres- the following estimation will be a good approach before mode failure occurs:

$$F_{\perp}^{\sigma} : \nu_{\perp\parallel} = \nu_{\perp\parallel(0)} \cdot E_{\perp(sec)} / E_{\perp(0)}$$

Also in the case of $F_{\perp\parallel}$ the value for $\nu_{\perp\parallel}$ is reduced.

7.6 Remarks on Design and Modelling

- In composite structures composed of stiff fibres and hopefully well-designed by netting theory the fibre net controls the strain behaviour.
- The FMC considers the interlaminar stresses and classifies the failure modes. Therefore, associated degradation models are inherent and make a gradual degradation of the affected property possible.
- In order to design a laminate properly, not only *verified* failure conditions have to be available, but also *proper* stresses have to be analytically provided⁴⁵. Therefore, analogous to isotropic materials, the nonlinear stress-strain curves have to be taken into account below reaching the initial failure level.
- Above the initial failure level an appropriate progressive failure analysis method has to be employed by taking a *Successive Degradation Model* and by using a failure mode condition that indicates failure type and quantifies damage danger or fracture risk.
- *Final failure* occurs after the structure has degraded to a level where it is no longer capable of carrying additional load. This is most often caused by FF, however in specific cases by IFF, too. An inclined wedge-shaped inter-fibre crack caused by F_{\perp}^{τ} can lead to final failure (Puc96)⁴².
- Multidirectional laminates are usually still capable of carrying load beyond *initial failure* which usually is determined by IFF.

8 CALCULATION PROCEDURE

Figure 9 presents a suitable flow chart of the nonlinear calculation. The solution procedure of the nonlinear analysis aims to establish static equilibrium on each load step after material

properties have been changed. For each iteration the procedure is repeated until convergence (equilibrium) is reached or total failure. A correction of the fibre angle in accordance with the change of the specimens geometry has been considered.

By employing the equivalent stress reached in each failure mode the associated secant modulus of each mode was determined for the hardening and the softening regime.

Considering a consistent stress concept for all $\sigma_{eq}^{(modes)}$ an *explicite* dependency for $E_{sec}(\sigma_{eq}^{(mode)})$ has to be provided. For reasons of achieving such an explicite formulation two separate formulae are discriminated which are linked in the strength point. This automatically respects that the chosen nonlinear calculation procedure ~~chosen~~ demands for the dependencies of the secant moduli on the corresponding equivalent stress. These dependencies are;

(example F_{\perp}^{τ}):—

- $\Delta\sigma > 0$ (increasing stress , hardening)

$$E_{\perp(sec)}^t = E_{\perp(o)}^t$$

$$E_{\perp(sec)}^c = E_{\perp(o)}^c / [1 + 0.002 \cdot (E_{\perp(o)}^c / R_{p0.2}^{\perp c}) \cdot (\sigma_{eq}^{\perp \tau} / R_{p0.2}^{\perp c})^{n_{\perp}^c - 1}] \quad (43)$$

$$G_{\parallel(sec)} = G_{\parallel(o)} / [1 + 0.002 \cdot (G_{\parallel(o)} / R_{p0.2}^{\perp \parallel}) \cdot (\sigma_{eq}^{\perp \parallel} / R_{p0.2}^{\perp \parallel})^{n_{\perp}^{\parallel} - 1}]$$

- $\Delta\sigma < 0$ (decreasing stress , softening)

$$E_{\perp(sec)}^t = \sigma_{eq}^{\perp \sigma} / \varepsilon(\sigma_{eq}^{\perp \sigma}) = (\sigma_{eq}^{\perp \sigma} / b_s^{\perp t}) / \left[\ln \left(\frac{R_{\perp}^t - \sigma_{eq}^{\perp \sigma}}{\sigma_{eq}^{\perp \sigma}} \right) - \frac{a_s^{\perp t}}{b_s^{\perp t}} \right]. \quad (44)$$

For the further modes the same formula is valid, however, the mode parameters are different. The eqns(44) may be transferred to Puck's degradation function η (see also Annex A1.2). After having reached $Eff^{(res)} = 1$ this value is kept in the further degradation procedure which causes a stress redistribution towards the fibres as far as the fibre net allows it. Thereby, also the residual stresses are reduced.

If the laminate's stiffness matrix is recomputed after each step of damage increase the laminate's damage evolution may be continuously monitored. The approach may be called a self-correcting secant modulus procedure.

9 APPLICATION TO TEST CASES

9.1 Definition of test cases

In the Tables 3 to 5 the properties for a CFRP and a GFRP laminate are presented. Table 6 provides a survey of the initial and final failure envelopes to be nonlinearly computed.

9.2 Assumptions and remarks for the plots

- *Post-initial failure* is considered by gradually degraded properties of embedded laminae (no Sudden Death of the failed lamina). The course of the softening (suffix s) is assumed
- First FF is *final failure*. The two FF F_{\parallel}^{σ} (tensile fibre failure) and F_{\parallel}^{τ} (shear instability, local buckling), and sometimes the IFF F_{\perp}^{τ} , are defined to cause *final failure*
- Failure mode identification according to Cuntze's definition is inherent to the Failure Mode Concept
- Parameters m , b_{\perp}^{τ} , $b_{\perp \parallel}$, and $b_{\perp \parallel}^{\tau}$ are roughly assumed for the given UD-test cases ~~examples~~
- Comment: As temperature drop the difference *stress free* temperature minus *room* temperature as *effective* temperature difference (Table 3) ~~is~~ is applied in order to consider the effect of ~~the~~ curing stresses (are residual stresses of the 1st kind)

Moisture ~~is~~ may be assumed here to have a balancing effect of 30°C. Chemical shrinking⁶ and thermal curing stresses do not affect the shear stresses.

Micromechanical curing stresses (residual stresses of the 2nd kind at filament/matrix level) could not be assessed and are not considered. They are assumed here to be respected in the values for the UD-strengths.

- The given stress-strain curves of the UD-lamina are interpreted mechanical load-based *macro-mechanical* stresses. It is assumed that the stress-strain curves are *mean* curves (\bar{R} – values are given), the type one needs for test data mapping (see Figures 5)
- An ~~Edge~~ edge effect (3D state of stress) is not considered, because the laminates are assumed to be part of a 'closed' composite structure
- A progressive behaviour of $E_{||}^t$ (valid for C-fibres, only) was not regarded (see Figure15)
- The loading is monotonic and proportional. No loading path effects are considered (should be considered some time):
- In respect of the few multiaxial lamina test data one single value $\dot{m} = 3.1 = \text{const}$ will be taken for the various 'test cases'.

For the computation of the *test cases* the following *failure conditions* will be employed (σ_3 is included only in the equations where they are effective):

$$\begin{aligned}
 \text{FF1,2: } & \frac{\varepsilon_1 \cdot E_{||}^t}{\text{Eff}^{\parallel\sigma} \cdot R_{||}^t} = 1; & \frac{-\sigma_1}{\text{Eff}^{\parallel\tau} \cdot R_{||}^c} = 1 \\
 \text{IFF1,2: } & \frac{\sigma_2}{\text{Eff}^{\perp\sigma} \cdot R_{\perp}^t} = 1; & \frac{\tau_{21}^3 + b_{\perp||} 2\sigma_2 \tau_{21}^2}{(\text{Eff}^{\perp||} \cdot R_{\perp||})^3} = 1 \\
 \text{IFF3: } & \frac{(b_{\perp}^{\tau} - 1)(\sigma_2 + \sigma_3) + b_{\perp}^{\tau} (\sigma_2 - \sigma_3)^2 + b_{\perp||}^{\tau} \cdot \tau_{21}^2}{\text{Eff}^{\perp\tau} \cdot R_{\perp}^c} + \frac{b_{\perp}^{\tau} (\sigma_2 - \sigma_3)^2 + b_{\perp||}^{\tau} \cdot \tau_{21}^2}{(\text{Eff}^{\perp\tau} \cdot R_{\perp}^c)^2} = 1
 \end{aligned} \tag{45}$$

~~wh~~Herein $\sigma_3 = -p_{\text{ex}}$ is to be inserted in the case of *tube specimens* loaded by external pressure p_{ex} , and for *flat specimens* holds $\sigma_3 = 0$. The consideration of $\sigma_3 = -p_{\text{ex}}$ shifts the biaxial strength capacity to higher values. In the modes IFF1 and 2 the pressure $\sigma_3 = -p_{\text{ex}}$ has no effect.

For the computation of the stress effort the particular 2D-state of stress ($\sigma_1, \sigma_2, \tau_{21}$) has to be inserted into the eqns(45). This will either not lead to failure, if $\text{Eff}^{(\text{mode})} < 1$, or to failure if $\text{Eff}^{(\text{mode})}$ is exceeding the value 1.

The modes IFF1 and IFF2 may be called harmless failures whereas IFF3 may cause a catastrophic failure which is respected in the nonlinear analysis.

The equivalent stress, building up the denominators, was defined by

$$\text{Eff} \cdot R = \sigma_{\text{eq}}(\{\sigma\}), \tag{46}$$

including the ~~A~~ residual stress ~~has to be included in~~ σ_{eq} by a superposition to the load stress according to

$$\{\sigma\} = \{\sigma\}_{(L)} + \{\sigma\}_{(R)} . \quad (47)$$

The residual stress is decaying with decreasing stiffness.

9.3 Stress-strain curves of the UD-lamina

On the following Figures **10** to **17** the course of the test data (solid lines) is displayed as well as the softening curve which is assumed for the embedded UD-lamina (dotted curve). One remark has to be added here: The dotted part of the F_{\perp}^{τ} -curve is only active if catastrophic failure of the 'delamination initiating' wedge (its oblique microcracks are still closed yet deliver some compliance) is prevented by the laminate.‡

9.4 Biaxial failure envelopes for the UD-lamina

In the following UD failure envelopes the *residual stresses* are not regarded. Thus, only the so-called *load stresses* from the mechanical load test are considered. For the nonlinear analysis the Ramberg/ Osgood exponent and the assumed softening parameters of eqn(40) are added to each capture.

The course of the presented test curves has been verified by tests at MAN and tests cited in literature (ZTL80⁴⁶, VDI976, ~~Kna72~~).

The Figures 5 and 18 to 22 depict several cross-sections of the five-dimensional IFF-body:

- *Fig. 5:* In the graphs (σ_2, σ_3) and (τ_{23}, σ_2) , the latter was not shown here, fracture may be excellently described by the homogenized stresses
- *Fig. 18:* The graph (τ_{21}, σ_2) represents the IFF-responsible stresses in the plane of the lamina; the graph (τ_{31}, σ_2) outlines that τ_{31} does not have the same action plane as σ_2^{\perp} (at first investigated by Puck, not derivable in Tsai/Wu's approach)
- *Fig. 19:* The graph (σ_2, σ_1) shows the limited applicability of the homogenized lamina stresses, because σ_1 or I_1 is not the fracture stress. This is the fibre stress σ_{1f} . In order to maintain the composite level in the graph the fibre stress is multiplied by the fibre volume fraction (approach: $\sigma_{1f} \cdot v_f = \varepsilon_1 \cdot E_{\parallel}^{\perp}$)
- *Fig. 20/21:* In the graph $(\sigma_2 = \sigma_3, \sigma_1)$ the peculiarities of a 2D lateral stressing are depicted. In the domain $\sigma_2^c = \sigma_3^c > -10R_{\perp}^c$ failure is caused, not by IFF, yet due to Poisson's effect by F_{\parallel}^{σ} . The zoom, Figure21, visualizes the rounding-off in one interaction domain ($F_{\perp}^{\sigma} / F_{\parallel}^{\sigma}$)
- *Fig. 22:* This graph eventually highlights the (τ_{21}, σ_1) -interaction.

9.5 Initial and final biaxial failure envelopes

For the determination of the failure envelopes (see Figures 23 to 26) the code Mathcad, nonlinear CLT, and an assumed softening behaviour were applied. The symbols used to indicate the mode of failure are the symbols which characterize the failure function, eg τ_{\parallel} for F_{\parallel}^{τ} and so on. The angle marks the associated lamina. A 'temperature drop' is not considered.

- *Fig. 23* incorporates the initial and the final failure envelope of this GFRP-laminae.

In the positive quadrant there are no corners. Generally, corners become smoothed due to the effect of high interaction of the failure modes. In the domain A-B both F_{\parallel}^{σ} in the two adjacent laminae are 'acting together'.

In the negative quadrant wedge failure may occur in the compressed laminate specimen. The event of a wedge failure is equal to the onset of delamination damage. In case of a plane laminate specimen, despite the antibuckling device applied when testing in the compression regime, the wedge will slide and then cause a compressive reaction σ_3^c normal to the lamina's plane onto the adjacent laminae (see Puck's drive shaft⁴²). This will induce delamination or

might increase an initial delamination size. However, in case of a pressure loaded *tension/compression-torsion tube specimen* (applied at MAN ; see also VDI976) and in case of *high pressure vessels* (1000 bar, ARIANE 5 launcher) loaded by external pressure p_{ex} the multiaxial strength is increased ($\sigma_3 = -p_{ex}$ is acting in a favourable manner). The sliding friction due to p_{ex} is increased similarly until its maximum will be reached.

Mind: A correct analysis of boundary conditions and stress state of the test specimen is mandatory before evaluating and applying the data.

- Fig. 24 depicts the symmetrical failure envelopes of this CFRP *laminae*. The sharp corners still have to be rounded-off in a refined procedure taking into account the joint failure probability of the *laminata* (Cun87)³⁸. In the negative quadrant IFF covers FF.

- The last two failure envelopes (Figures 25 and 26) are concerning the $[90 / +30 / -30]_s$ -laminata subjected to a $(\hat{\sigma}_x, \hat{\sigma}_y)$ state of stress and a $(\hat{\tau}_{xy}, \hat{\sigma}_x)$ state of stress. Again here, sharp corners should be rounded there where the joint failure probability of the failure modes comes to act.

9.6 Stress-strain curves of the laminates

The following stress-strain curves (Figures 27 to 33) consider the eqns (45) and the data from the Tables³ 3 and 6. The loading is monotonic, a temperature drop from curing (would cause an off-set) is not regarded.

Figure 27 and 28 outline the deformation behaviour of a pressure vessel, which is usually designed for one special load case 'inner pressure' that means for $\hat{\sigma}_y / \hat{\sigma}_x = 2:1$.

Load combinations outside of this ratio - such as 1:0 (Fig. 27) - will lead to too high shear strains and thereby to a 'limit of usage' (l.u.). This shear strain *design limit* or limit of usage was assumed here to be $\max \gamma = 4\%$ shear strain which corresponds more or less to the shear fracture strain of the isolated lamina.

As the authors were asked to provide the text with more test data (Figure 34) was added.

10 SOME CONCLUSIONS, OUTLOOKS

10.1 Regarding the FMC-based conditions

- A general concept was highlighted for the establishment of Failure Conditions ($F = 1$) for *Initial Failure* (corresponding to IFF) of dense, brittle laminae and Final Failure of the laminata
- The *complete* failure surface consists of piecewise smooth regimes (partial failure surfaces). Each regime represents *one failure mode* and is governed by *one basic strength*
- Sufficient for pre-dimensioning are the basic strengths R . The remaining unknown *curve parameters* $b_{\perp\parallel}$, b_{\perp}^{τ} , $b_{\perp\parallel}^{\tau}$ can be estimated if test data are not available. The rounding-off exponent m , after some fitting experience, can be fixed on the safe side by taking a little *lower* value
- The *interaction* (rounding-off) of *adjacent failure modes* is automatically considered when calculating the stress effort $Eff^{(res)}$ as function of the mode efforts $Eff^{(modes)}$
- The concept enables to correctly turn the design key by respecting the most critical mode and the location (Cun98)^{25,29} in the Finite Element idealization of the structure (Annex 4)
- ~~The solution procedure (Mathcad applied) worked in the failure exercise~~
- Homogenization of the UD-material comes to its limit if a *constituent* stress governs the failure. This is the case for F_{\parallel}^{σ} , where the macromechanical stress σ_1 has to be replaced by the actual fibre stress σ_{1f} . A fibre stress may be zero not even for zero σ_1 ; therefore ~~it~~ σ_{1f} has to be ~~assessed~~ estimated as $\sigma_{1f} = \varepsilon_1 \cdot E_{1f}$. In order to

remain on *composite* stress visualization level σ_{1f} will be multiplied by the fibre volume fraction v_f

- The 'mode fit' avoids the shortcomings of the 'global fit' which maps the course of test data by mathematically linking failure modes which are in reality not mechanically linked. One typical shortcoming is, that a reduction of the strength of one mode ~~will~~ might increase the multiaxial strength in another (independent) mode or part of the global failure surface.
- For the prediction of final failure the initial failure approach is not of that high concern, if wedge failure, caused by $F_{\perp}^{\tau} < 1$ and followed by delamination failure, will not occur (see A. Pucks drive shaft⁴² or torsion spring)
- Each failure condition describes the interaction of stresses affecting the same failure mode and assesses the actual state of stress in a 'material point'
- For (σ_2, σ_3) states of stress Mohr's stresses, Mohr's envelope curve, and the inclined fracture angle θ_{fp} may be determined
- Damage mechanics is captured in the FMC conditions so far as the stiffness reduction is determinable via the $(\sigma_{eq}, \varepsilon)$ -curve, and by the predictability of delamination initiation, applying F_{\perp}^{τ} and F_{\perp}^{σ}
- Regarding the investigations in theory and test carried out in Germany on the *lamina* material level in the last years (still going on) the understanding has improved a lot and seems to be a good basis to tackle *laminates* stacked-up of UD-laminae and fabric laminae. For other textile preforms (3D, stitched etc.) *engineering models* have to be developed.
 - The transferability to rhombically-orthotropic composites (fabrics) works (Cun98)^{27,28}.
- The choice of linear or other ~~forms~~ terms of ~~conditions in~~ stress invariants is based on whether there are volume and/or shape changes of the material element as well as on curve fitting considerations.
- In respect of the scatter of the actual test data the parameter set $b_{\perp}^{\tau} = 1, b_{\perp||} = b_{\perp||}^{\tau} = 0$ will often be an approach good enough for *final* failure analysis of the laminate.

10.2 Regarding the 'failure exercise'

- In the failure exercise both parts of a failure theory are necessarily compared in a combined manner: The physically and/or geometrically nonlinear stress analysis together with the applied failure conditions. Because it is not only a competition of the predictive capabilities of the failure conditions, the judging of the failure theories without viewing the nonlinear stress analysis would be only the half of the story.
- If a part of the predicted initial or final failure envelope should not match the test results this may be caused by the many assumptions to be made, too.
- Instability of the laminate is regarded as excluded, because the exercise is a strength failure exercise
- Material testing: In order to completely understand the material behaviour also for the constituent matrix the (σ, ε) -curve, biaxial failure stress envelopes and informations on lamina porosity should be depicted. Biaxial failure stress envelopes for the same matrix material in literature show contradictions!
Of course, in future testing has to verify the degradation assumptions made.

LITERATURE

1. Hinton, M.J., Soden, P.D. and Kaddour, A.S.: Comparison of Failure Prediction Methods for Glass/Epoxy and Carbon/Epoxy Laminates under Biaxial Stress. *ICCM11, Vol. V, 672-682 (1997)*
2. Hinton, M.J., Soden, P.D. and Kaddour, A.S.: Failure Criteria in Fibre-Reinforced-Polymer Composites . Special Issue, *Composites Science and Technology 58 (1998)*
3. Soden, P.D., Hinton, M.J. and Kaddour, A.S.: Lamina Properties, Lay-up Configurations and Loading Conditions for a Range of Fibre-reinforced Composite Laminates. Special Issue, *Composite Science and Technology 58 (1998), 1011-1022*

4. Soden, P.D., Hinton, M.J. and Kaddour, A.S.: A Comparison of the Predictive Capabilities of Current Failure Theories for Composite Laminates. Special Issue, *Composites Science and Technology* 58 (1998), 1225-1254
5. Knappe, W. und Schneider, W.: Bruchkriterien für unidirektionalen Glasfaser-Kunststoff unter ebener Kurzzeit- und Langzeitbeanspruchung". *Kunststoffe*, Bd. 62, 1972, 864-868
6. (VDI97) Cuntze, R.G., et.al.: Neue Bruchkriterien und Festigkeitsnachweise für unidirektionalen Faser-kunststoffverbunde unter mehrachsiger Beanspruchung – Modellbildung und Experimente -. VDI-Fortschrittbericht, Reihe 5, Nr. 506 (1997, 250 pages)
7. Herrmann, G.: Zum Bruchverhalten gerichteter Glasfaserverbunde. *Dissertation*, TU-Stuttgart, Inst. f. Werkstoffe im Bauwesen, 1982
8. Puck, A.: Calculating the strength of glass fibre/plastic laminates under combined load. *Kunststoffe, German Plastics (German Plastics is the bilingual English and German edition of Kunststoffe)*, 1969, 55, 18-19 (in German, pp. 780-787).
9. Puck, A. and Schneider, W.: On failure mechanisms and failure criteria of filament-wound glass-fibre/resin composites. *Plast. Polym.*, 1969, Feb., 33-43.
10. Puck, A.: Praxisgerechte Bruchkriterien für hochbeanspruchte Faser-Kunststoffverbunde. *Kunststoffe* 82 (1992) 2, S. 149-155 (Fracture Criteria for highly Stressed Fibre Plastics Composites which Meet Requirements of Design Practice. *Kunststoffe German Plastics* 82 (1992) 2, p.36-38)
11. Puck, A.: Faser-Kunststoff-Verbunde mit Dehnungs-oder Spannungs-Kriterien auslegen? *Kunststoffe* 82 (1992) 5, S. 431-434 (Should Fibre-Plastics Composites be Designed with Strain or Stress Criteria? *Kunststoffe German Plastics* (1992) 5, P. 34-36)
12. Puck, A.: Ein Bruchkriterium gibt die Richtung an. *Kunststoffe* 82 (1992) 7, S. 607-610 (A failure criterion shows the Direction – Further Thoughts on the Design of Laminates-. *Kunststoffe German Plastics* 82 (1992) 7, p. 29- 32)
13. Hashin, Z.: Failure Criteria for Unidirectional Fibre Composites. *J. of Appl. Mech.* 47 (1980), 329-334
14. Cuntze, R.G.: A Physically based 2D/3D-Inter-Fibre-Failure Criterion for brittle UD-layers – Hashin's idea and Puck's realization -. Key-note lecture, *ISODUR 93, Porto, July 18-21*
15. Jeltsch-Fricker, R.: Bruchbedingungen vom Mohrschen Typ für transversal-isotrope Werkstoffe am Beispiel der Faser-Kunststoff-Verbunde. *ZAMM* 76 (1996), 505-520
16. Jeltsch-Fricker, R. und Meckbach, S.: "Fast Solver of a Fracture Condition According to Mohr for Unidirectional Fibre-Polymer Composite" (in German), *Scripts of the University of Kassel on Appl.Math.*, No. 1/96
17. Michaeli, W. And Huybrechts, D. : A New Approach for the Dimensioning of Thick Laminates using Physically based Strength Criteria. *Proc. 39th Conf. of the Society for the Advancement of Material and Process Engineering (SAMPE)*, Vol.2, 11-14 April 1994, Anaheim,CA, pp.2829-2840
18. Huybrechts, D.: Ein erster Beitrag zur Verifikation des wirkebenebezogenen Zwischenfaserbruchkriteriums nach Puck. *Dissertation an der RWTH Aachen*, 1996
19. Rackwitz, R. and Gollwitzer, S.: A New Model for Inter-Fibre-Failure of high strength Unidirectionally Reinforced Plastics and its Reliability Implications. *NATO-workshop PROBAMAT-21*. Century, Perm, Russia, Sept. 10-12, 1997
20. Kopp, J. and Michaeli, W.: Dimensioning of Thick Laminates using New IFF Strength Criteria and some Experiments for their Verification. *Proceedings "Conf. on Spacecraft Structures Materials and Mechanical Testing"*, ESA, 27-29 March 1996
21. Kopp, J. and Michaeli, W.: The New Action Plane related Strength Criterion in Comparison with Common Strength Criteria, *Proceedings of ICCM-12*, Paris, France, July 1999
22. Hufenbach, W. and Kroll, L.: A New Failure Criterion Based on the Mechanics of 3-Dimensional Composite Materials. *ICCM-10*, Whistler, Canada, 1995
23. Cuntze, R.G.: "Fracture-type Strength Criteria" formulated by Invariants which consider the Materials Symmetries of the Isotropic/Anisotropic Material used. *Conf. on Spacecraft Structures, Materials and Mechanical Testing. ESA-CNES-DARA: Noordwijk*, March 1996 (*Conf. Hdbk*)
24. Cuntze, R.G.: Evaluation of Multiaxial Test Data of UD-laminae by so-called "Fracture Type Strength Criteria" and by supporting Probabilistic Means. *ICCM-11*, Gold Coast, Australia, 1997
25. Cuntze, R.G. and Sukarie, G.: Effective Dimensioning of 3D-stressed UD-laminae on Basis of Fracture-type Strength Criteria. *Int. conf. on Mechanics of Composite Materials*. Riga, April 20-23, 1998. *Conference handbook*, Presentation
26. Cuntze, R.G.: The Failure Mode Concept - A new comprehensive 3D-strength Analysis Concept for Any Brittle and Ductile behaving Material. *Europ. Conf. on Spacecraft Structures, Materials and Mechanical Testing. ESA-CNES-DGLR-DLR; Braunschweig*, Nov. 1998, *ESA SP-428*, 269-287
27. Cuntze, R.G.: Strength Prediction for Multiaxially Loaded CMC-Materials. *3rd European Workshop on thermal Protection Systems. ESA-ESTEC: Noordwijk*, March 1998, WP P141
28. Cuntze, R.G.: Application of 3D-strength criteria, based on the so-called "Failure Mode Concept", to multiaxial test data of sandwich foam, concrete, epoxide, CFRP-UD lamina, CMC-Fabric Lamina. *ICCE/5*, Las Vegas, July 1998 (presentation)

29. Cuntze, R.G.: Progressive Failure of 3D-stressed Laminates: Multiple Nonlinearity treated by the Failure Mode Concept (FMC). DURACOSYS 99, Brussels, July 1999,
30. Boehler, J.P.: Failure Criteria for Glass-Fiber Reinforced Composites under Confining Pressure. *J. Struct. Mechanics* 13 (1985), 371
31. Boehler, J.P.: Personal note to the first author on Fabric Invariants, 1995
32. Jeltsch-Fricker, R. and Meckbach, S.: A parabolic Mohr Fracture Condition in Invariant Formulation for Brittle Isotropic Materials (in German). *ZAMM*, 79 (1999), 465-471
33. Meckbach, S.: Invariants of Cloth-reinforced Fibre Reinforced Plastics. *Kasseler Schriften zur angewandten Mathematik, Nr. 1/1998 (in German)*
34. Christensen, R.M.: The Numbers of Elastic Properties and Failure Parameters for Fiber Composites. *Transactions of the ASME, Vol. 120 (1998), 110-113*
35. Cuntze, R.G.: Deterministic and Probabilistic Prediction of the Distribution of Inter-Fibre Failure Test Data of Prestrained CFRP Tubes composed of Thin Layers and loaded by radial pressure. Wollongong. *Advanced Composites '93, 579-585. The Minerals, Metals & Materials Society, 1993*
36. Grimmelt, M. and Cuntze, R.G.: Probabilistic Prediction of Structural Test Results as a Tool for the Performance Estimation in Composite Structures Design. Beuth Verlag, *VDI-Bericht 771 (1989), 191-200*
37. Rackwitz, R. and Cuntze, R.G.: System Reliability Aspects in Composite Structures. *Eng.' Opt., 1987, Vol. 11, pp. 69-76*
38. Cuntze, R.G.: "Failure Path Analysis of Multilayered Fibre Reinforced Plastic Components with the Reliability Calculation Programme FRPREL". *Noordwijk, Oct. 1987*
39. Mohr, O.: Welche Umstände bedingen die Elastizitätsgrenze und den Bruch eines Materials? *Civilingenieur XXXIV (1900), 1524-1530, 1572-1577*
40. Flaggs, D.L. and Kural, M.H.: "Experimental Determination of the In Situ Transverse Lamina Strength in Graphite Epoxy Laminates". *J. Comp. Mat. Vol 16 (1982), S. 103-116*
41. Masters, J.: Fractography of Modern Engineering Materials. Composites and Metals. 2nd volume. *ASTM STP1203, 1994*
42. Puck, A.: Festigkeitsanalyse von Faser-Matrix-Laminaten - Modelle für die Praxis -. München: *Carl Hanser Verlag, 1996*
43. Awaji, H. and Sato, S.: A Statistical Theory for the Fracture of Brittle Solids under Multiaxial Stresses. *Intern. Journal of Fracture* 14 (1978), R13-16
44. MiL Hdbk 17 Plastics for Aerospace Vehicles. Vol I "Reinforced Plastics"; Vol. II; Vol. III "Utilization of Data." Dep. of Defence (DOD), USA
45. Rolfes, R., Noor, A.H. and Rohwer, K.: Efficient Calculation of Transverse Stresses in Composite Plates. *MSC-NASTRAN User Conference, 1997*
46. (ZTL80) Dornier, Fokker, MBB, DLR: Investigations of Fracture Criteria of Laminae. 1975-1980, Grant from German ministry, BMVg. (multiaxial testing, reports in German)
47. Puck, A. and Schürmann, H.: Failure Analysis of FRP Laminates by Means of Physically based Phenomenological Models. Special issue of "*Composite Science and Technology*" 58 (1998),
48. Paul, B.: A modification of the Coulomb-Mohr Theory of Fracture. *Journal of Appl. Mechanics* 1961, p.259-268
49. Christensen, R.M.: Stress based Yield/ Failure Criteria for Fiber Composites. *Int. J. Solids Structures* 34. (1997), no. 5, 529-543
50. Christensen, R.M.: Yield Functions/Failure Criteria for Isotropic Materials. *Proc. R. Soc. Lond. A (1997) 453, 1473-1491*
51. Hart-Smith, L.J.: An Inherent Fallacy in Composite Interaction Failure Curves. *Designers Corner, Composites* 24 (1993), 523-524
52. Goldenblat, I.I., Kopnov, V.A.: Strength of Glass-reinforced Plastics in the complex stress state. *Polymer Mechanics of Mechanical Polimerov, Vol. 1 1966, 54-59*
53. Thom, H.: A Review of the Biaxial Strength of Fibre-Reinforced Plastics. *Composites Part A* 29 (1998), 869-886
54. Tsai, S.W. and Wu, E.M.: A General Theory of Strength for Anisotropic Materials. *Journal Comp. Mater, Vol. 5 (1971), 58-80*
55. Yeh, H.Y. and Kilfoy, L.T.: A Simple Comparison of Macroscopic Failure Criteria for Advanced Fiber Reinforced Composites. *J. of Reinforced Plastics and Composites, Vol. 17 (1998), 406-445*
56. Wang, J.Z.: Failure Strength and Mechanism of Composite Laminates under Multiaxial Loading Conditions. Dissertation, Univ. of Illinois at Urbana, 1993
57. Rowlands, R.E.: Strength (Failure) Theories and their Experimental Correlation. In Sih, G.C. Skudra, A.M., Editoren, *Handbook of Composites, Band III, Kapitel 2*, Elsevier Science Publisher B.V., Madison, WI, U.S.A., 1985, 71-125

58. Matzenmüller, A., Lubliner, J., Taylor, R.L.: A constitutive model for Anisotropic Damage in Fiber Composites. *Mechanics of Materials* 20 (1995), 125 – 152
59. Sukarie, G.: Einsatz der FE-Methode bei der Simulation des progressiven Schichtversagens in laminierten Faserverbundstrukturen. *Symposium "Berechnung von Faserverbundstrukturen unter Anwendung numerischer Verfahren"*. München, Techn. Univ., 13./14. März 1996
60. Slight, D.W., Knight, N.F. and Wang, J.T.: Evaluation of a Progressive Failure Analysis Methodology for Laminated Composite Structures. 38th Structure, Structure Dynamic and Material Conference, April 1997. *AIAA Paper* 97-1187
61. Puck, A.: Physically based IFF-criteria allow realistic strength analysis of fibre-matrix-laminates. (In German), *Proceedings of the DGLR-Conference 1996*, Ottobrunn, Germany, 1997, pp. 315-352

Acknowledgement

The authors gratefully express their thanks for the intensive collaboration with Prof. A. Puck reviewing this paper in the context with the comparison of the two approaches. The authors also thank the reviewers for their constructive comments.

ANNEXES

A1 Comparison of Puck's and Cuntze's failure theories

A1.1 – Comparison of Puck's fracture plane based IFF-criteria and Cuntze's FMC-based invariant ——formulations

~~This~~ The two sections ~~is~~ A1.1 and A1.2 are a common formulation of Puck and Cuntze, because both authors have often been asked for an explanation of the coincidences and differences between ~~the two~~ their approaches. The following should be mentioned in this context:

- With respect to the different effort that has been put by Puck et al (incl. Cuntze) into the fracture plane based criteria and by Cuntze into the FMC based criteria the 'Puck criteria' are approaching the 'series status' and the 'Cuntze criteria' only the 'development status'.
- The FMC criteria seem to be generally applicable to all materials. Therefore, there are a few short comings in their application to UD-material.

As early as 1968/69 Puck concluded from experimental observations, that two completely different types of fracture should be distinguished and theoretically treated by separate failure criteria: Fibre Failure (FF) and Interfibre Failure (IFF)^{8,9} (~~Puc69a,69b~~). In the early seventies the discrimination of these two fracture types became common practice in the German aerospace industry⁴⁶ (~~ZTL80~~). In all later papers of Puck and Cuntze the separate treatment of FF and IFF has been maintained.

For FF both authors use simple maximum stress criteria, based on the consideration, that the composite fails when the fibres reach a certain critical stress.

Both authors feel that for the new anisotropic fibres a better approach for FF prediction may be necessary.

Since another fundamental paper of 1992 (Puc92)¹², research in Germany has concentrated on the improvement of IFF criteria. This appeared to be of higher importance than assumed in the past after it had been learned from experience on torsional tube springs, that the wedge effect of oblique fractures under transverse compression can cause destruction of the whole composite part (~~Puc98~~)⁴⁷. Besides this, under alternating loads, microcracks, due to IFF (caused mainly by transverse tensile stress), give rise to high peaks of interlaminar stresses which initiate local delaminations.

Common foundation of the two approaches:

The failure theories of Puck and Cuntze are based on the same fundamental assumptions:

- The UD-layer is transversally-isotropic and failure occurs by brittle fracture.
- Mohr's statement is valid: The material strengths are determined by the stresses on the fracture plane.

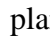
- The fracture plane may be inclined with respect to the plane which the external stresses are acting on. (This is, for instance, true for uniaxial transverse compression.)
- For states of stress without longitudinal shear (τ_{31}, τ_{21}), that means plane stress conditions consisting of a stress state ($\sigma_2, \sigma_3, \tau_{23}$) which can be replaced by ($\sigma_{II}, \sigma_{III}$), the so-called principal stresses ($\sigma_{II}, \sigma_{III}$) of the transversally-isotropic plane, both authors make the same assumption:

Paul's modification of the Coulomb-Mohr theory of fracture (Pau61)³⁹ is valid. This is based on the assumption, that two different modes of fracture can occur which leads to the following fracture hypothesis (analogous-formulation analog to that for isotropic material):

'An intrinsically brittle material will fracture in either that plane where the shear stress τ_{nt} reaches a critical value which is given by the shear fracture resistance $R_{\perp\perp}^A$ of a fibre parallel plane increased by a certain amount of friction. This friction is caused by the simultaneously acting compressive stress σ_n on that plane. Or, it will fracture in that plane, where the maximum principal stress (σ_{II} or σ_{III}) reaches the transverse tensile strength R_{\perp}^t ' (FigureA1/1 and A/2).

Results for plane stress ($\sigma_{II}, \sigma_{III}$)

For this state of stress without any longitudinal shear (τ_{31}, τ_{21}) there is a complete coincidence of the formulations of Puck and Cuntze.

The treatment of this problem by Mohr's circle (representing the state of stress (σ_n, τ_{nt}), on any plane, see  FigureA1/1 and Mohr's fracture envelope (representing the fracture limit for combined (σ_n, τ_{nt})-stresses) is well known.

- For the domain $\sigma_n < 0$ Puck⁴² starts with the assumption of a parabolic fracture envelope $\tau_{nt} = \tau_{nt}(\sigma_n)$ for $\sigma_n < 0$ [Puc98]:

$$\tau_{nt}^2 = (R_{\perp\perp}^A)^2 - 2p_{\perp\perp}^{(-)} R_{\perp\perp}^A \sigma_n \quad (A1)$$

wherein $R_{\perp\perp}^A$ is the transverse shear fracture resistance of a fibre parallel plane against its fracture caused by 'friction coefficient' for $\sigma_n < 0$.

At fracture Mohr's circle and the fracture envelope have a common point of contact, that means the same inclination $d\tau_{nt}/d\sigma_n$. From this condition the fracture angle Θ_{fp} between the action plane of σ_{II} and the fracture plane can be calculated, which is varying a little with the difference of ($\sigma_{II} - \sigma_{III}$),

$$\cos 2\Theta_{fp} = -\cos 2\Theta_{fp}^c \frac{R_{\perp}^c}{\sigma_{II} - \sigma_{III}} \quad (\text{for } \sigma_n < 0) \quad (A2)$$

with Θ_{fp}^c = fracture angle under uniaxial transverse compression (angle between the action plane of the uniaxial compressive stress σ_{II} and the corresponding fracture plane which is $45^\circ < |\Theta_{fp}^c| < \approx 60^\circ$) and R_{\perp}^c = transverse compression strength. In this equation σ_{II} and σ_{III} are stresses at fracture!:-

By means of this result a definite form in $\sigma_{II}, \sigma_{III}$ for the fracture condition is found which is parabolic and invariant in the transversal plane:

- ~~Cuntze in contrast to Puck Cuntze starts with this invariant formulation~~

$$F_{\perp}^{\tau} = \frac{a_{\perp}^{\tau}}{R_{\perp}^c} (\sigma_{II} + \sigma_{III}) + \frac{b_{\perp}^{\tau}}{(R_{\perp}^c)^2} (\sigma_{II} - \sigma_{III})^2 = 1. \quad (A3)$$

- Cuntze in contrast to Puck starts already with this invariant formulation (A3).

The adaptation to ~~the~~ experimental uniaxial compression results (strength R_{\perp}^c and fracture angle Θ_{fp}^c) gives $a_{\perp}^{\tau} = b_{\perp}^{\tau} - 1$ and $b_{\perp}^{\tau} = 1 / (2 \cos 2\Theta_{fp}^c + 1)$ (A4) (~~or see chapter 4~~). In eqn(21b) another adaption of b_{\perp}^{τ} to test results is shown.

Puck's and Cuntze's approach for the domain $\sigma_n < 0$ are connected by the relation (A2) for the fracture angle Θ_{fp} .

For the domain $\sigma_n \geq 0$ both authors use the 'tensile cut-offs' recommended by Paul⁴⁸. That means that the fracture stress is either $\sigma_{II} = R_{\perp}^t$ or $\sigma_{III} = R_{\perp}^t$, see Figure 5 or A 1/2.

Results for states of stress with additional longitudinal shear (τ_{31}, τ_{21})

In this field the two authors use rather different approaches:

- Puck stays with the ~~the more or less~~ 'physically based' consideration of the mechanical interaction of the stresses $\sigma_n, \tau_{nt}, \tau_{n1}$ on the fracture plane (Figure A1/3). He uses simple polynomials (parabolic or elliptic) to formulate a master-fracture body in ~~the~~ the $(\sigma_n, \tau_{nt}, \tau_{n1})$ -stress space.

Starting from this (master-) fracture body generally no analytical solutions can be found for the fracture angle Θ_{fp} (with the exception of $(\sigma_1, \sigma_2, \tau_{21})$ -states of stress) and therefore no analytical solutions can be given for the fracture bodies in $\sigma_1, \sigma_2, \sigma_3, \tau_{23}, \tau_{31}, \tau_{21}$.

Therefore, the necessary search for the fracture plane, that means for the plane with the lowest reserve factor $\min f_{Res}(\Theta)$ or the highest stress exposure factor $\max f_E(\Theta)$, has to be done numerically (using the formulation of the fracture condition in $\sigma_n, \tau_{nt}, \tau_{n1}$) in an angle range between $-90^\circ \leq \Theta \leq +90^\circ$. By means of the ~~lowest~~ f_{Res} found fracture angle Θ_{fp} , resulting from the numerical procedure, the stresses $(\sigma_1, \sigma_2, \dots, \tau_{21})$ at fracture can be calculated by multiplying the acting stresses $(\sigma_1, \sigma_2, \tau_{21})$ by the lowest reserve factor $\min f_{Res}(\Theta) = f_{Res}(\Theta_{fp})$.

The numerical search for the fracture plane is an inconvenience, but on the other hand the user of this approach automatically gets an information on the fracture angle and on the "fracture mode". Puck defines the 'fracture mode' as the stress combination $(\sigma_n, \tau_{nt}, \tau_{n1})$ or $(\sigma_{\perp}, \tau_{\perp\perp}, \tau_{\perp\parallel})$ on the fracture plane. For the calculation of the fracture stresses Cuntze's invariant formulation is of course the more convenient one.

The results can be visualized by fracture bodies in a 3-dimensional $(\sigma_{II}, \sigma_{III}, \tau_{\omega 1})$ -space, where $\tau_{\omega 1}$ is the "resultant" of τ_{31} and τ_{21} . These fracture bodies are not symmetric with respect to the $(\sigma_{II} = \sigma_{III})$ -plane²¹.

- Cuntze uses three simple invariant formulations in $(\sigma_1, \sigma_2, \tau_{21})$ ~~1~~ one linear, ~~1~~ one quadratic and ~~1~~ one cubic polynomial- which lead to fracture bodies in the $(\sigma_{II}, \sigma_{III}, \tau_{\omega 1})$ space similar to those of Puck. He feels that ~~(micro-)~~ mechanical and probabilistic interactions can not be clearly distinguished and therefore he models the 'mode' interactions by a simple probabilistic series model ('rounding-off' procedure achieved by the determination of $f_{Res}^{(res)}$ or $Eff^{(res)}$).

Attention has to be paid to the fact that the expression 'mode' has different meanings in the papers of Puck and Cuntze. Puck differentiates between 7 interfibre fracture (sub)-modes M1 to M7 (according to the number of the possible ~~possible stress combinations~~ acting on the fracture plane) which may be allocated to the three Modes A, B, C (see Fig. A1/4):

Group with $\sigma_n \geq 0$

$$\begin{aligned}
&M1 = (\sigma_{\perp}^t, \tau_{\perp\perp}, \tau_{\perp\parallel}) \text{ the most general mode} \\
&\left. \begin{aligned}
&M2 = (\sigma_{\perp}^t, 0, 0) \\
&M3 = (\sigma_{\perp}^t, 0, \tau_{\perp\parallel}) \\
&M4 = (0, 0, \tau_{\perp\parallel})
\end{aligned} \right\} \text{ Domain of Mode A}
\end{aligned} \tag{A5}$$

Group with $\sigma_n < 0$

$$M5 = (\sigma_{\perp}^c, 0, \tau_{\perp\parallel}) \quad \text{Domain of Mode B}$$

$$\left. \begin{aligned}
&M6 = (\sigma_{\perp}^c, \tau_{\perp\perp}, \tau_{\perp\parallel}) \\
&M7 = (\sigma_{\perp}^c, \tau_{\perp\perp}, 0)
\end{aligned} \right\} \text{ Domain of Mode C.}$$

$$\begin{aligned}
&\text{---} \text{1.) } (\sigma_{\perp}^t, \tau_{\perp\perp}, \tau_{\perp\parallel}); \text{ 2.) } (\sigma_{\perp}^t, 0, 0); \\
&\text{---} \text{3.) } (\sigma_{\perp}^t, 0, \tau_{\perp\parallel}); \text{ 4.) } (0, 0, \tau_{\perp\parallel}); \text{ 5.) } (\sigma_{\perp}^c, 0, \tau_{\perp\parallel}); \\
&\text{---} \text{6.) } (\sigma_{\perp}^c, \tau_{\perp\perp}, \tau_{\perp\parallel}); \text{ 7.) } (\sigma_{\perp}^c, \tau_{\perp\perp}, 0).
\end{aligned} \tag{A5}$$

---Cuntze uses the expression 'mode' to address his three different invariant IFF conditions, based on the idea that for each of these fracture conditions in their 'pure' regimes either the σ_{\perp} -, the $\tau_{\perp\perp}$ -, or the $\tau_{\perp\parallel}$ -stressing is "'dominant'".

---Of course, one has to pay for the higher convenience of the invariant approach with a certain loss of 'physical correctness' and the inability to predict the fracture angle for states of stress including longitudinal shear τ_{21}, τ_{31} ". ~~;~~ ~~but~~ However, this may be acceptable in many cases of design practice.

A1.2 Comparison of Puck's and Cuntze's failure analysis of laminates

This section focusses on a 2D-laminate failure analysis as performed in the 'failure exercise', Part A³.

For fibre failure (FF) of the UD-lamina both authors use the same simple maximum stress failure criterion:

$$f_E^{(FF)} = \frac{\sigma_1}{R_{\parallel}^t} = 1 \quad \text{for } \sigma_1 \geq 0 \quad \text{and} \quad f_E^{(FF)} = \frac{-\sigma_1}{R_{\parallel}^c} = 1 \quad \text{for } \sigma_1 < 0 \quad . \tag{A6}$$

f_E is the stress exposure factor used by Puck. It has essentially the same meaning as Cuntze's resultant stress effort $\text{Eff}^{(res)}$. The value of f_E or $\text{Eff}^{(res)}$, respectively, quantifies the 'risk of fracture'. Fracture occurs, if $f_E = 1 = 100\%$.

Both authors also assume that FF in at least one lamina of a laminate means final failure of the laminate.

Therefore, the biaxial failure envelopes for final failure of laminates predicted by the two authors do not differ very much, as long as the laminates have three or more fibre directions. The strengths of these laminates are 'fibre dominated'.

Also, the predicted stress/strain curves of such laminates look very similar because the fibres which are much stiffer than the matrix carry the main portion of the loads. Different degradation procedures after the onset of interfibre failure (IFF) do therefore not influence the predicted strains very much. This is especially true for CFRP laminates.

Puck's degradation procedure (known as the η -degradation) for the secant moduli $E_{2(sec)}$ and $G_{21(sec)}$ after the onset of IFF is rather simple, since Puck's IFF-criteria are completely based

on the assumption of a mechanistic interaction of σ_2 and τ_{21} . Probabilistic aspects can be dealt with, if necessary, in a separate operation⁴².

In Puck's theory the numerical search for the fracture angle θ_{fp} , that means the search for the stress action plane with the highest angle dependent stress exposure factor $\max f_E^{(IFF)}(\theta)$, is not necessary in the special case of a *plane state of stress* $(\sigma_1, \sigma_2, \tau_{21})$. For tensile $\sigma_2 > 0$ and also for moderate compressive stress ($|\sigma_2| < 0.4 R_{\perp}^c$) the fracture plane is the same as the action plane of σ_2 and τ_{21} , Figure A1/4. That means: $\theta_{fp} = 0$. For rather high compressive stresses ($|\sigma_2| > 0.4 R_{\perp}^c$) the fracture angle $\theta_{fp} \neq 0$ can be calculated from a very simple analytical expression:

$$\theta_{fp} = \arctan \sqrt{\frac{R_{\perp\perp}^A}{-\sigma_2}} . \quad (A7)$$

Attention! In this equation σ_2 is the compressive stress at fracture caused by a combined (σ_2, τ_{21}) state of stress.

Based on the knowledge of the fracture angle there have been found three simple analytical expressions for the stress exposure factor $f_E^{(IFF)}$ formulated with σ_2 and τ_{21} instead of $\sigma_n, \tau_{nt}, \tau_{n1}$. Each of the three equations is valid for a certain region of the (σ_2, τ_{21}) -fracture curve)^{42,47}:

- Mode A is valid for $\sigma_2 \geq 0$ and combines the modes M2, M3, M4 mentioned in eqn(A5)
- Mode B is valid for $0 \leq |\sigma_2/\tau_{21}| \leq R_{\perp\perp}^A / |\tau_{21}^c|$ and is identical with mode M5.
- Mode C is valid for the region with $\theta_{fp} \neq 0$, i.e. $0 \leq |\tau_{21}/\sigma_2| \leq |\tau_{21}^c| / R_{\perp\perp}^A$ and combines the modes M6 and M7.

One should remember that the expression 'mode' has different meanings in the papers of Puck and Cuntze! Puck's stress exposure factors $f_E^{(IFF)}$ for his Modes A, B and C are not equivalent to Cuntze's mode efforts $\text{Eff}^{(\text{mode})}$ but to Cuntze's $\text{Eff}^{(\text{res})}$! Like $f_E^{(IFF)}$ also $\text{Eff}^{(\text{res})}$ quantifies the risk of fracture due to the combined action of σ_2 and τ_{21} .

Puck's fracture condition for IFF of a UD-lamina is

$$f_E^{(IFF)} = 1 . \quad (A8)$$

For a UD-lamina in a laminate, this means the onset of progressive IFF ('matrix cracking') the three different equations for $f_E^{(IFF)}$ are (Figure A1/4):

$$\text{- For Mode A: } f_E^{(IFF)} = \frac{1}{R_{\perp\parallel}} \cdot \left[\sqrt{\tau_{21}^2 + \left(\frac{R_{\perp\parallel}}{R_{\perp}^t} - p_{\perp\parallel}^{(+)} \right)^2 \sigma_2^2} + p_{\perp\parallel}^{(+)} \sigma_2 \right] , \quad (A9)$$

$$\text{- For Mode B: } f_E^{(IFF)} = \frac{1}{R_{\perp\parallel}} \cdot \left(\sqrt{\tau_{21}^2 + p_{\perp\parallel}^{(-)} \sigma_2^2} + p_{\perp\parallel}^{(-)} \sigma_2 \right) , \quad (A10)$$

$$\text{- For Mode C: } f_E^{(IFF)} = \frac{R_{\perp}^c}{4(R_{\perp\parallel} + p_{\perp\parallel}^{(-)} R_{\perp\perp}^A)^2} \cdot \frac{\tau_{21}^2}{(-\sigma_2)} + \frac{(-\sigma_2)}{R_{\perp}^c} . \quad (A11)$$

Hence, for Mode A the fracture angle θ_{fp} is 0° and, because σ_2 is a tensile stress, the micro cracks tend to open. The resulting decrease of the secant moduli $E_{2(sec)}$ and $G_{21(sec)}$ is modelled by Puck by a simultaneously starting degradation of $E_{2(sec)}$ and $G_{21(sec)}$. That means, secant moduli $\eta E_{2(sec)}$ and $\eta G_{21(sec)}$ with $\eta < 1$ are used after the onset of IFF. The degradation factor η is a decaying function decreasing with increasing load, in order to keep $f_E^{(IFF)} = 1$. After the onset of IFF only 'average stresses' can be calculated for a microcracked lamina. Average stresses are defined as stresses smeared over some length of the cracked lamina (which includes a number of microcracks).

After the onset of IFF, Puck calculates the average stresses $\sigma_2(\eta)$ and $\tau_{21}(\eta)$ by using $\eta E_{2(sec)}$, $\eta G_{21(sec)}$, and $\eta \nu_{12}$. He assumes that in the progressive cracking process of a lamina its average stresses $\sigma_2(\eta)$ and $\tau_{21}(\eta)$ remain approximately constant with increasing load. This is achieved in the calculation by keeping $f_E^{(IFF)} = 1 = \text{constant}$ after the first IFF has occurred.

- In contrast to Puck's completely $f_E^{(IFF)}$ -controlled η -degradation Cuntze uses his 'stress exposure factor' $\text{Eff}^{(res)}$ (or f_E) only for a certain correction, in order to take into account mode-interactions. His degradation is mainly controlled by using the $\sigma_2(\varepsilon_2)$ - or the $\tau_{21}(\gamma_{21})$ -stress/strain curve for finding the valid secant modulus $E_{2(sec)}$ or $G_{21(sec)}$, respectively. The branches with increasing stresses ('hardening') of these stress/strain curves are found by the usual experiments with uniaxial σ_2 -stress or pure τ_{21} -stress, respectively. The branches with rapidly decreasing stresses (called 'softening') are preliminarily assumed, see Figures 10 to 17. Like Puck, Cuntze calculates the stresses σ_2 and τ_{21} in the laminae of the laminate by using secant moduli from the $\sigma_2(\varepsilon_2)$ - and $\tau_{21}(\gamma_{21})$ -stress/strain curves. However, Cuntze has to pay attention to a proper interaction of the interactive modes in the stress and strain analysis in the following manner: In order to take into account the combined probabilistic/mechanistic interaction of the failure modes the secant moduli $E_{2(sec)}$ and $G_{21(sec)}$ are taken from the $\sigma_2(\varepsilon_2)$ -curve or the $\tau_{21}(\gamma_{21})$ -curve not just at the stresses σ_2 or τ_{21} resulting from the stress and strain analysis for the actual level load. Their values are taken at a little higher stress in the 'hardening branch' with increasing stress and at a little lower stress in the 'softening branch' with decreasing stress. This 'stress correction' is controlled by the so-called 'triggering approach', which is described in chapter 6, see eqns(35) and (36). The controlling parameter is the ratio of the resultant stress exposure factor $\text{Eff}^{(res)}$ to the maximum mode exposure factor $\text{maxEff}^{(mode)}$. By this triggering approach lower secant moduli $E_{2(sec)}$ and $G_{21(sec)}$ are provided for the next calculation loop as those which would result without the correction by the triggering approach.

The Figures A1/5 and A1/6 visualize Puck's η -degradation and Cuntze's 'triggering approach'. In Cuntze's theory for the actual load the degradation of $E_{2(sec)}$ and $G_{21(sec)}$ is performed with the same trigger factor TrF. In contrast to Puck's theory, if one of the corrected equivalent mode stresses has reached its strength level, a rapid decrease of the mode's average (smeared over the microcracks) equivalent stress will follow. There is another difference: Cuntze's triggering approach is already active before the onset of IFF. This can perhaps be justified by the fact that there is a certain mutual interaction of σ_2 and τ_{21} on their strains before the fracture stresses have been reached, see fig.1 in literature⁴⁷.

Due to the severe lack of experimental experience about the real degradation of laminates after IFF initiation different authors make very divergent assumptions about the average stresses in a lamina after the onset of IFF until final failure of the laminate, as can be seen from the 'failure exercise'⁴. The Figures A1/5 to A1/6 demonstrate this for the two authors Puck and Cuntze.

In order to demonstrate the different assumptions most drastically the case is considered where compressive σ_2 does *not* lead to a premature final failure due to the wedge effect. Because of the assumption that for compressive σ_2 the cracks stay closed after IFF initiation Puck does not degrade E_{2s} and ν_{12} . Therefore a rapid η -degradation of τ_{21} alone has to keep $f_E^{(IFF)} = 1$. In contrast to this Cuntze treats the compressive stress σ_2 similar to a tensile stress σ_2 with a pronounced softening branch of the stress/strain diagram (Figure11). He is basing this approach on weakening effects due to the cracking.

Both authors are aware of the fact that up to now there is a severe lack of experimental experience about the 'real' degradation processes in FRP-laminates. It is much to be hoped that the 'failure exercise' and further research will promote knowledge in this field.

A2A2 Additional Biaxial (σ_2, τ_{21}) -Test Data for UD-laminae

Figure34 provides with additional test data for one GFRP and one CFRP material (VDI97). As test specimen the wound 'tension /compression - torsion tube specimen' was used.

A3 Visualization of the Reserve Factors of a Uniformly Loaded Sandwich Plate –

In this annex a still existing example (Table A3/1) is taken in order to visualize the 'handling' with the values computed for $f_{Res}^{(mode)}$ and $f_{Res}^{(res)}$ (further see Table A3/2) .

Failure conditions and corresponding curve parameters are not depicted here, because they belong to a slightly different former set of fracture conditions (Cun98)²⁶. But, the following results nevertheless highlight how the designer will work with reserve factors or with efforts.

The listing of the reserve factors values in Table A3/2 completely describes the stress situation in all the laminae, with (k) indicating the particular lamina. Numbers in quadratic brackets refer to the finite element (the FE code MARC was employed).

Lamina $k = 3$ contains the minimum resultant reserve factor (0.82), $\min f_{Res}^{(mode)}$, which is due to the 90°-angle still a little smaller than that for the 45°-lamina ($k = 2$) for which Figure A3/1 is prepared. This plot depicts the distribution of the resultant reserve factor for the lamina ($\alpha = +45^\circ$, $k = 2$) of the sandwich plate. Its smallest value 0.89 is lower than 1, thus indicating IFF which would cause a redesign if IFF is not permitted. The IFF is caused by σ_\perp^t in the lamina's plane and is critical over a large domain of the lamina.

Similar to f_{Res} Table A3/2 can be filled in by the various Eff. A clear determination of the design driving $\max Eff^{(mode)}$ would then be pointed out, too.

A4 A4 Further Simplifications of the FMC-based Failure Conditions

- Simplification of F_\perp^τ :

—As still briefly mentioned, the F_\perp^τ condition may be homogenized (I_4 is not homogeneous to I_2) in the form

$$F_\perp^\tau = (b_\perp^\tau - 1) \frac{I_2}{R_\perp^c} + b_\perp^\tau \frac{\sqrt{I_4}}{R_\perp^c} = 1, \quad (A6A12)$$

which means a replacing of I_4 by $\sqrt{I_4}$ and of setting $b_{\perp\parallel}^\tau = 0$. Then, the curve parameter b_{\perp}^τ may be simply determined from the equation

$$b_{\perp}^\tau = \frac{1 + (\sigma_2^{c\tau} + \sigma_3^{c\tau}) / \bar{R}_{\perp}^c}{\sqrt{(\sigma_2^{c\tau} + \sigma_3^{c\tau}) / \bar{R}_{\perp}^c + (\sigma_2^{c\tau} - \sigma_3^{c\tau})^2 / \bar{R}_{\perp}^{c2}}} \quad (\text{A7A13})$$

This value is different to that of the former b_{\perp}^c , of course.

Now, the reserve Factor-factor is linearly computable due to

$$f_{\text{Res}}^{\perp\tau} = R_{\perp}^c / (b_{\perp}^\tau - 1)I_2 + b_{\perp}^\tau \sqrt{I_4} \quad (\text{A8A14})$$

- Determination of $\max I_3^{3/2}$ for the *case discrimination* :

The limit for the applicability of $F_{\perp\parallel}$ for the given state of stress (marked by a dot) is

$$\frac{I_3^{3/2}}{I_2 I_3 - I_5} \leq \chi \cdot b_{\perp\parallel} ,$$

with a preliminary to be confirmed $\chi = 1.1$.

From the ratio above the limiting maximum value on the failure surface can be deduced via

$$I_3^{3/2} + b_{\perp\parallel}(I_2 I_3 - I_5) = R_{\perp\parallel}^3 ,$$

$$\frac{I_3^{3/2}}{(I_2 I_3 - I_5)} + b_{\perp\parallel} \cdot 1 = \frac{R_{\perp\parallel}^3}{(I_2 I_3 - I_5)} ,$$

$$\chi \cdot b_{\perp\parallel} + b_{\perp\parallel} = R_{\perp\parallel}^3 / \max(I_2 I_3 - I_5) . \quad (\text{A15})$$

From $\max(I_2 I_3 - I_5)$ follows

$$\max I_3^{3/2} = R_{\perp\parallel}^3 - b_{\perp\parallel} \max(I_2 I_3 - I_5) . \quad (\text{A16})$$

- Further simplification of $F_{\perp\parallel}$ (*recommendation*):

Also for $F_{\perp\parallel}$ a simplification is proposed

$$-F_{\perp\parallel} = \left(\sqrt[3]{2I_3} + b_{\perp\parallel} \sqrt[3]{I_2 I_3 - I_5} \right) ,$$

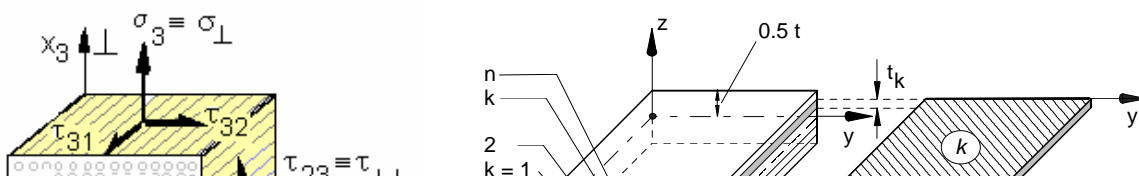
$$f_{\text{Res}}^{\perp\parallel} = R_{\perp\parallel} / \left(\sqrt[3]{2I_3} + b_{\perp\parallel} \sqrt[3]{I_2 I_3 - I_5} \right) \quad (\text{A17})-(\text{A9})$$

for later studies (see chapter 5.4). It should eliminate the afore mentioned possible numerical problem of $F_{\perp\parallel}$ and is therefore the *recommendation for the future*.

A5 The $(\tau_{21}, \sigma_2, \sigma_3)$ - Failure Body

The most interesting *partial IFF body* is that for the stress combination $(\tau_{21}, \sigma_2, \sigma_3)$. By this failure body (a difficult and time consuming work to produce it) the main differences of the new IFF conditions are displayed : This is at first the difference between (τ_{21}, σ_2) and (τ_{21}, σ_3) , see the typical asymmetry outlined in various papers of Puck et al.. According to the rounding procedure the $(\tau_{21}, \sigma_3^t = R_{\perp}^t)$ front side is not fully vertical anymore as by Puck documented. Nevertheless it provides with the main informations. Secondly the rounding-off in the (σ_2, σ_3) - (σ_2^t, σ_3^t) -domain is depicted.

The postprocessing of the failure body has caused some smaller irregularities and should be reworked with a better tool.



$$R_{\parallel}^t (= X^t), R_{\parallel}^c (= X^c), R_{\perp\parallel} (= S), R_{\perp}^t (= Y^t), R_{\perp}^c (= Y^c);$$

$$E_{\parallel}, E_{\perp}, G_{\parallel\perp}, \nu_{\parallel\parallel}, \nu_{\perp\perp}$$

Fig. 1. UD lamina

(t: = tension, c: = compression).

mid plane: $z = 0$

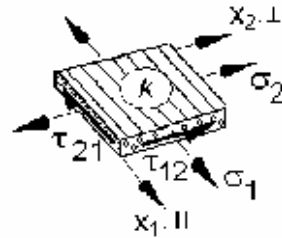


Fig. 2. Laminate and k' th lamina subjected to a plane state of stress (midplane $z = 0$)

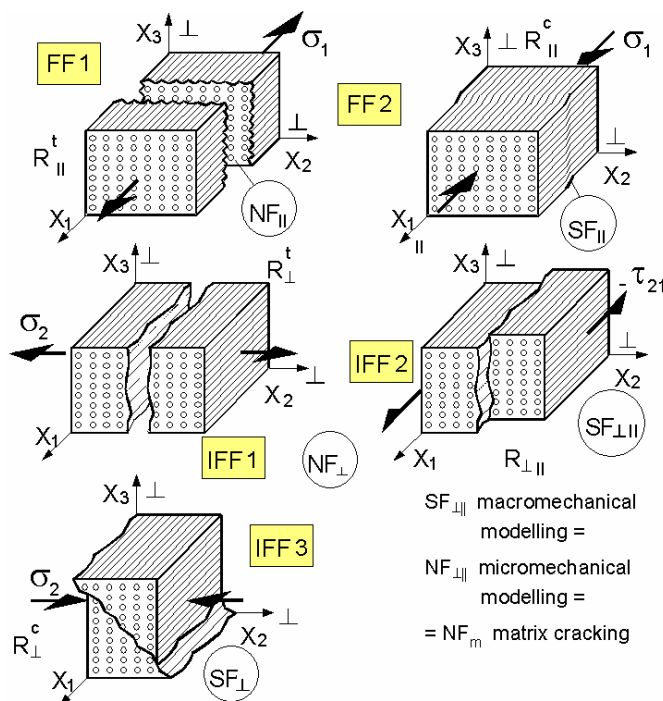


Fig. 3. FMC view of the fracture types (\equiv failure modes) of brittle transversally-isotropic material. (The physical fracture "planes" are pointed out in the figure (Cun98b) Θ_{fp} : = fracture plane angle). The onset of hackles due to NF_m relates IFF2 to IFF1 (microcracks due to NF_m)

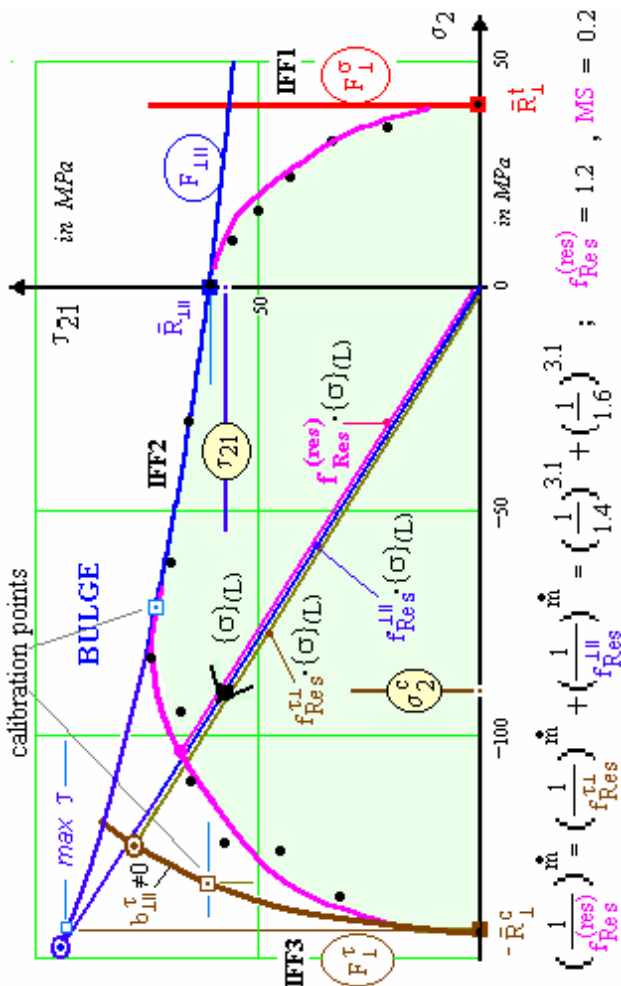
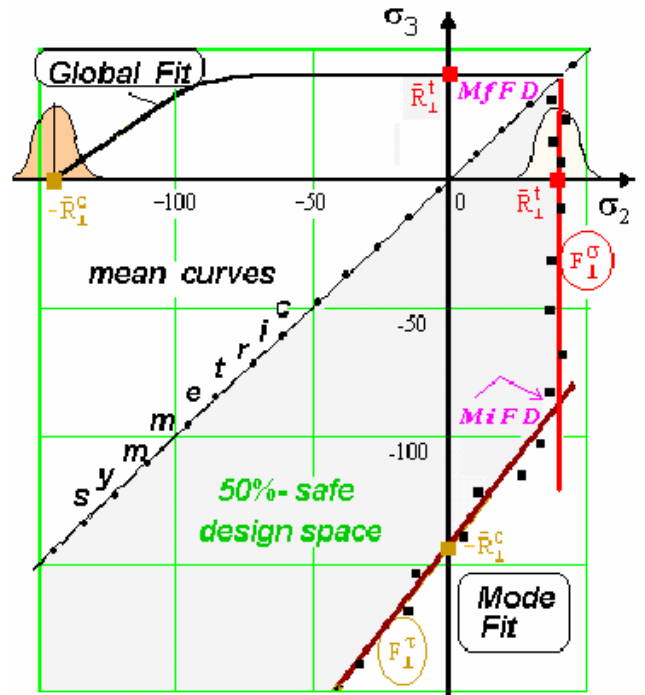
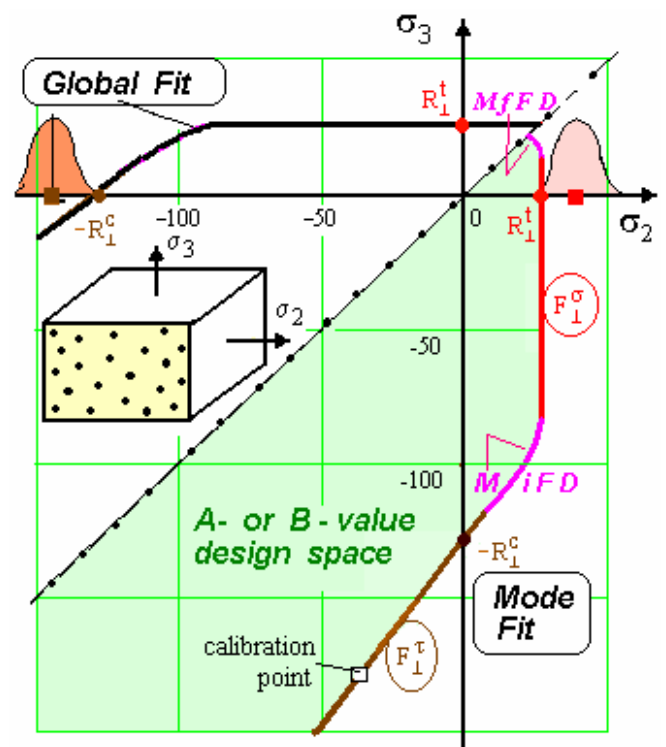


Fig. 4. Visualization of the reserve factor and computation example. $\{\sigma\}(L)$: = load stress vector, \dot{m} : = round-ing-off exponent. Eqns(45)



a) Test data evaluation with determination of curve parameters incl. strengths



b) Rounding-off in the MfFD, MiFD

Fig. 5. ‘Global Fit’ and ‘Mode Fit’. Scheme. Example: CFRP-IFF-curve of UD-material. (MiFD: = mixed failure domain = fracture due to 2 modes. MfFD: = multi-fold failure domain of the same mode "Normal Fracture" NF_{\perp} working twice. A-curve: 99% reliability, 95 % confidence ³⁴ B-curve: 90% / 95%, mean-curve: 50% / 50%). In A-, B-design space: $\bar{R} \rightarrow$ 'strength allowable' R

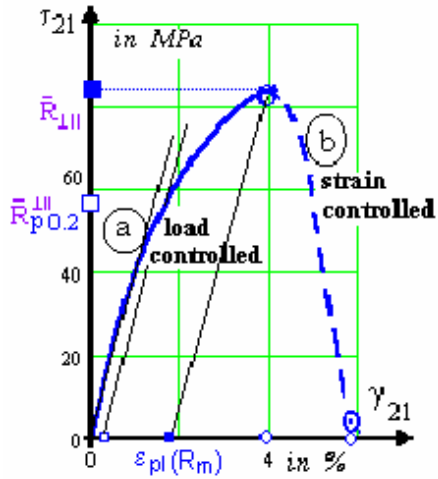


Fig. 6. Mapping of measured stress-strain curves of an isolated UD-specimen. Eqn(37) and eqn(40). (Example $\tau_{21}(\sigma_2)$)

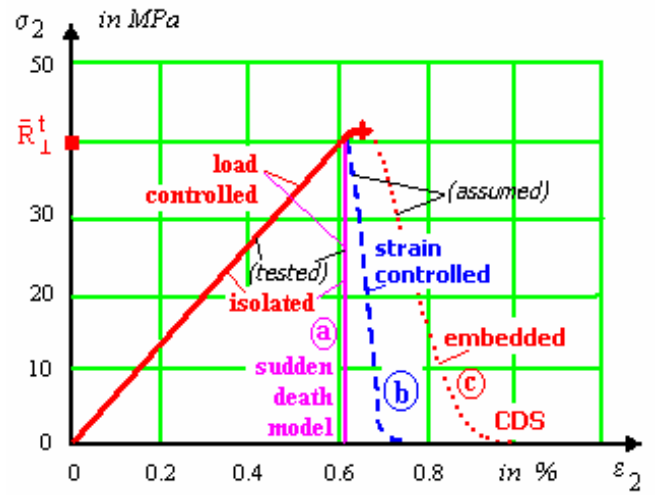


Fig. 7. The differences in the stress-strain behaviour of isolated and embedded UD-laminae. (For the (b)- and (c)-curve the eqn(40) is applied. The parameters for (b) and (c) are different.)

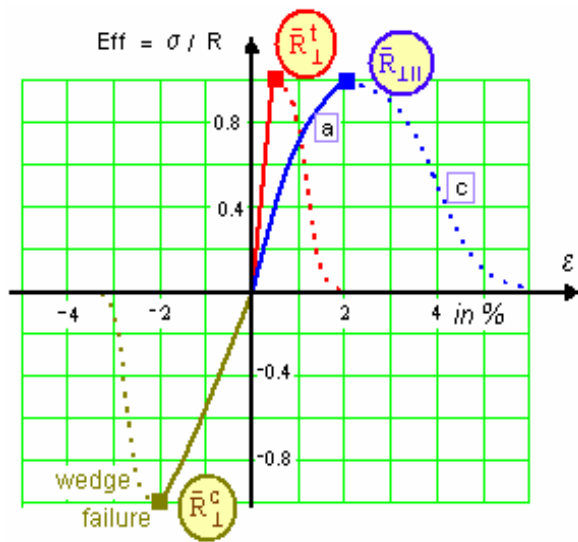


Fig. 8. Normalized stress-strain curves

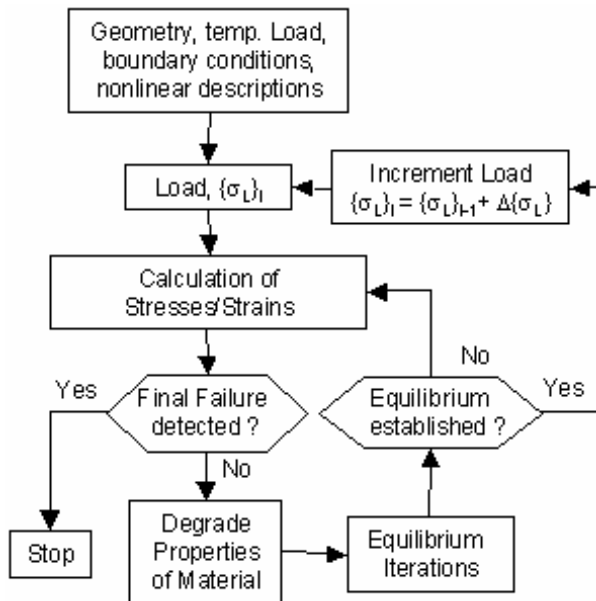


Fig. 9. Nonlinear calculation scheme (chosen)

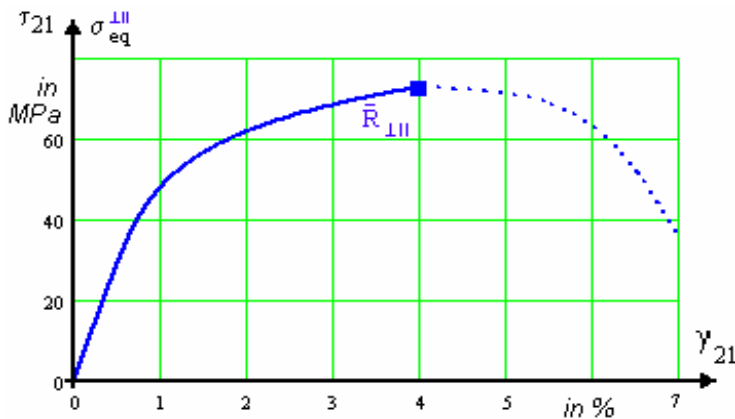


Fig. 10. In-plane shear stress-strain curve $\tau_{21}(\gamma_{21})$; UD-lamina (softening parameters assumed) GFRP: E-glass/MY750/HY917/DY063³. $\bar{R}_{\perp||} = 73$ MPa, $\bar{G}_{\perp||0} = 5.83$ GPa; $n^{\perp||} = 6.6$; $a_s^{\perp||} = -7.0\%$, $b_s^{\perp||} = 0.53\%$ (assumed)

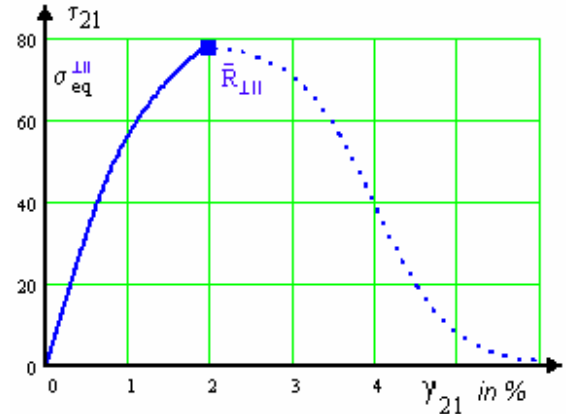


Fig. 13. In-plane shear stress-strain curve $\tau_{21}(\gamma_{21})$; UD-lamina (softening parameters assumed) CFRP: AS4/3501-6 epoxy³. $\bar{R}_{\perp||} = 79$ MPa, $\bar{G}_{\perp||0} = 6.6$ GPa; $n^{\perp||} = 5$; $a_s^{\perp||} = -4.0\%$, $b_s^{\perp||} = 0.46\%$

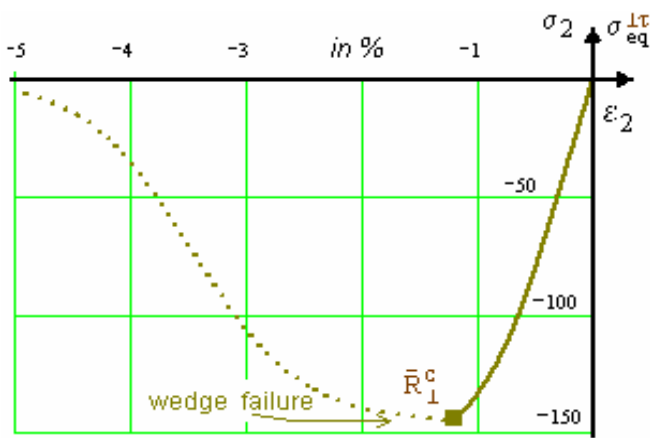


Fig. 11. Transv. compr. stress/strain curve $\sigma_2^c(\varepsilon_2)$; UD-lamina (softening parameters assumed). GFRP: E-glass/MY750/HY917/DY063³. $\bar{R}_{\perp}^c = 145$ MPa, $\bar{E}_{\perp0}^c = 16.2$ GPa; $n^{\perp c} = 6.6$; $a_s^{\perp c} = -3.45\%$, $b_s^{\perp c} = 0.47\%$

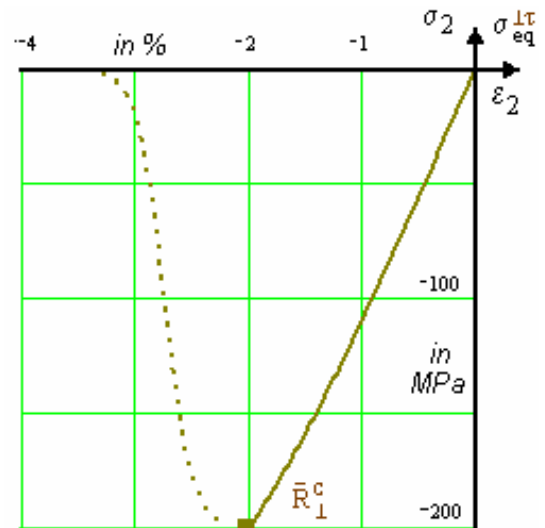


Fig. 14. Transv. compr. stress/str. curve $\sigma_2^c(\varepsilon_2)$; UD-lamina (softening parameters assumed). CFRP: AS4/3501-6 epoxy³. $\bar{R}_{\perp}^c = 200$ MPa, $\bar{E}_{\perp0}^c = 11$ GPa; $n^{\perp c} = 5$; $a_d^{\perp c} = -2.7\%$, $b_d^{\perp c} = 0.12\%$

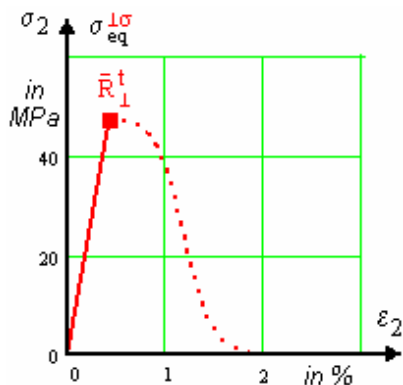


Fig. 12. Transv. tensile stress/strain curve $\sigma_2^t(\varepsilon_2)$; UD-lamina (softening assumed). CFRP: AS4/3501-6 epoxy³. $\bar{R}_{\perp}^t = 48$ MPa, $\bar{E}_{\perp0}^t = 11$ GPa; $a_s^{\perp t} = -1.2\%$, $b_s^{\perp t} = 0.15\%$;

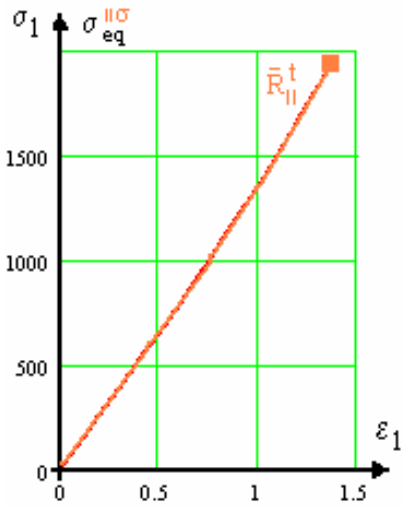


Fig. 15. Longit. tensile stress/strain curve $\sigma_1^t(\epsilon_1)$; UD-lamina. CFRP: AS4/3501-6 epoxy³.
 $\bar{R}_{\parallel}^t = 1950 \text{ MPa}$, $\bar{E}_{\parallel 0}^t = 126 \text{ GPa}$;

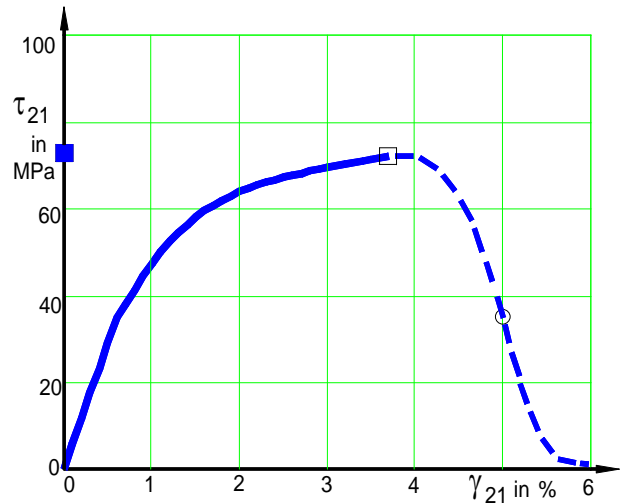


Fig. 16. In-plane shear stress-strain curve $\tau_{21}(\gamma_{21})$; UD-lamina (degradation assumed). E-glass/LY556/HT907/DY063³.
 $\bar{R}_{\perp\parallel} = 72 \text{ MPa}$, $\bar{G}_{\parallel\perp 0} = 5.83 \text{ GPa}$;
 $n^{\perp\parallel} = 5$; $a_s^{\perp\parallel} = -7.0\%$, $b_s^{\perp\parallel} = 0.54\%$

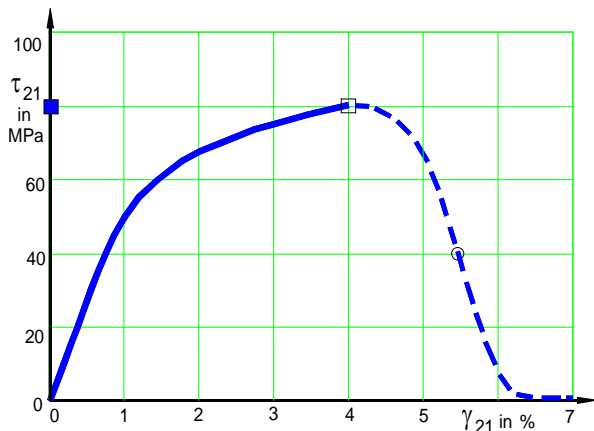


Fig. 17. In-plane shear stress-strain curve $\tau_{21}(\gamma_{21})$; UD-lamina (degradation assumed). T300/BSL914C epoxy³. $\bar{R}_{\perp\parallel} = 80 \text{ MPa}$, $\bar{G}_{\parallel\perp 0} = 5.5 \text{ GPa}$; $n^{\perp\parallel} = 5$; $a_s^{\perp\parallel} = -7.0\%$, $b_s^{\perp\parallel} = 0.53\%$

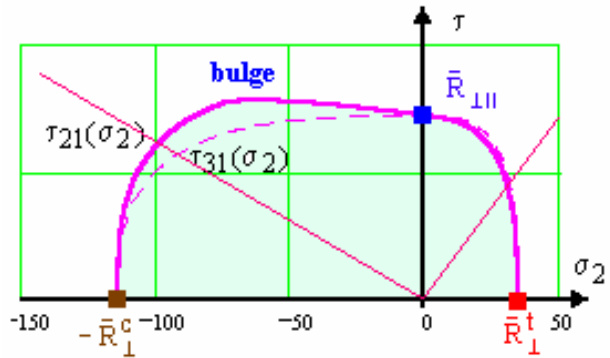


Fig. 18. Biaxial failure stress envelope (τ_{21}, σ_2) and (τ_{31}, σ_2) in MPa. UD-lamina . GFRP: E-glass MY 556 epoxy³
 $b_{\perp}^{\tau} = 1.5, b_{\perp\parallel} = 0.13, b_{\perp\parallel}^{\tau} = 0.4, \dot{m} = 3.1$. Eqn(45).
 (further data VDI97⁶, Kna72⁵)

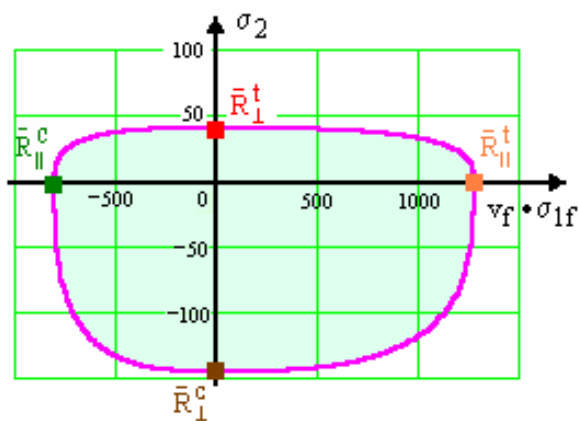


Fig. 19. Biaxial fail. stress envelope $(\sigma_2, v_f \sigma_{1f})$ in MPa. UD-lamina. E-glass / MY750 epoxy³ Eqn(45).
 $b_{\perp}^{\tau} = 1.56, b_{\perp\parallel} = 0.12, b_{\perp\parallel}^{\tau} = 0.4, \dot{m} = 3.1$.
 (further data: see eg (ZTL80)⁴⁶)

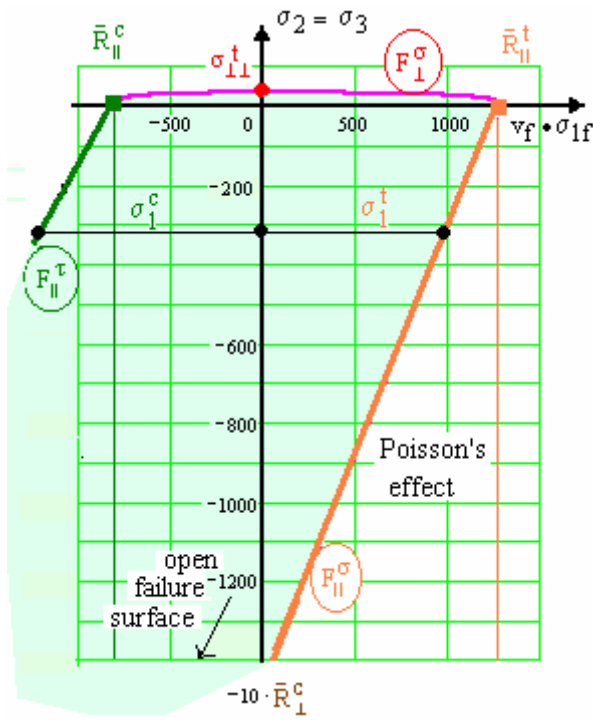


Fig. 20. Biaxial failure stress envelope ($\sigma_2 = \sigma_3, v_f \cdot \sigma_{1f}$); $\sigma_{\perp\perp}^t \approx R_{\perp}^t / \sqrt{2}$ in MPa. UD-lamina E-glass / MY750 epoxy³.
 $b_{\perp}^{\tau} = 1.56, b_{\perp\parallel} = 0.12, b_{\perp\parallel}^{\tau} = 0.4, \dot{m} = 3.1$. Eqn(45)

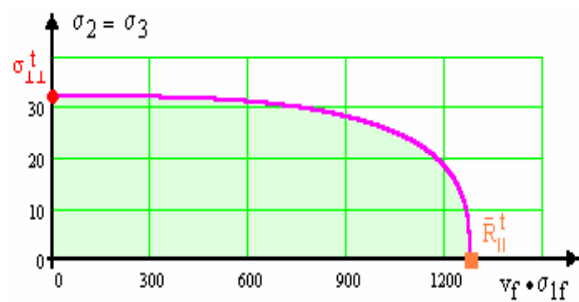


Fig. 21. Zoom of Fig. 20

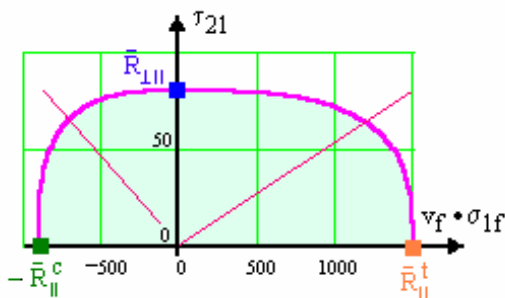


Fig. 22. Biaxial fail. stress envelope $\tau_{21}(v_f \sigma_{1f})$ in MPa. UD-lamina T300/BSL914C epoxy³.
 $b_{\perp}^{\tau} = 1.53, b_{\perp\parallel} = 0.15, \dot{m} = 3.1$. Eqn(45).
 See also (ZTL80)⁴⁶

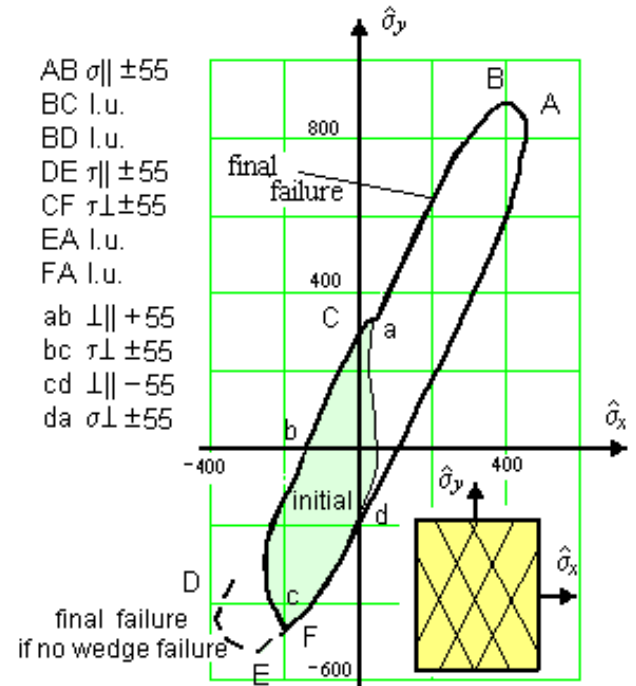


Fig. 23. Initial and final failure envel. $\hat{\sigma}_y(\hat{\sigma}_x)$. [+55/-55]_s-laminate, E-glass / MY750 epoxy³
 $b_{\perp}^{\tau} = 1.5, b_{\perp\parallel} = 0.13, b_{\perp\parallel}^{\tau} = 0.4, \dot{m} = 3.1$, Eqn(45)
 $\hat{\sigma}_y$:= average hoop stress of the laminate, x:= 0° direction. Limit of usage (l.u.) at $\gamma = 4\%$

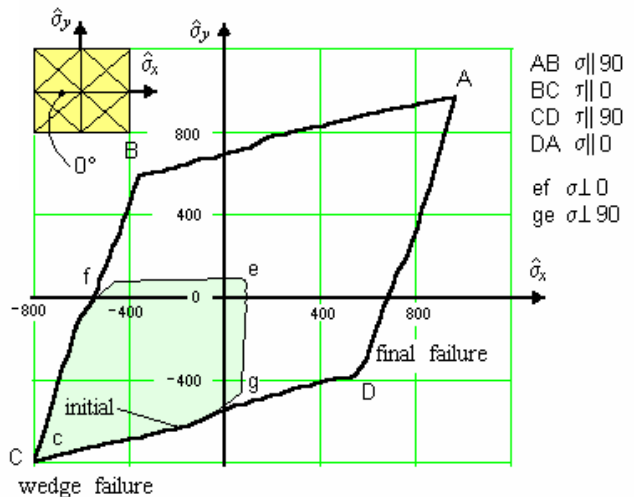


Fig. 24. Initial and final failure envel. $\hat{\sigma}_y(\hat{\sigma}_x)$ in MPa. [90/+45/-45/0]_s-laminate, AS4/3501-6³. Eqn(45)

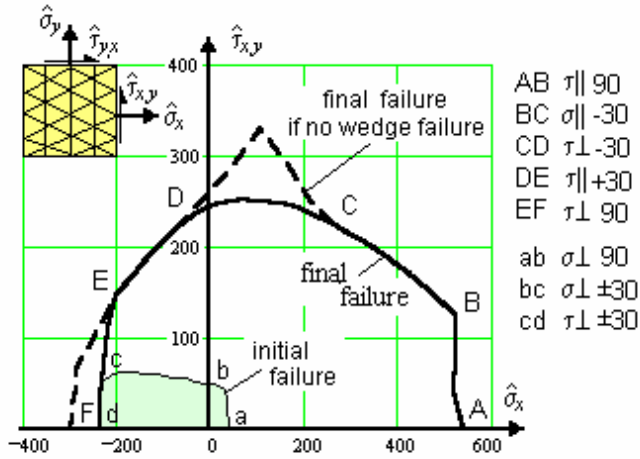


Fig. 25. Initial and final biaxial failure envel. $\hat{\tau}_{xy}(\hat{\sigma}_x)$.
 [90/+30/-30]_s-laminate. E-glass / LY556 epoxy³.
 $\hat{m} = 3.1$. Eqn(45)

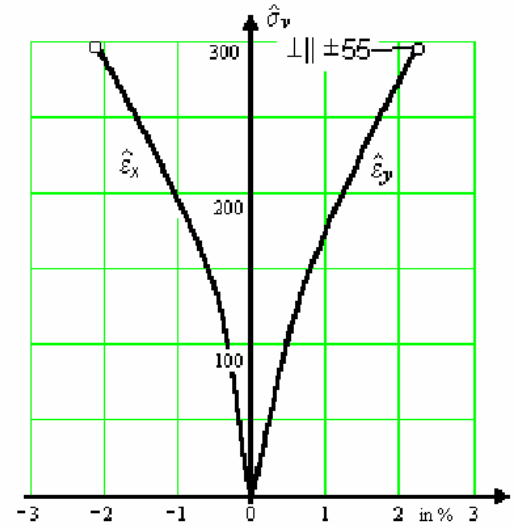


Fig. 27. Stress-strain curves $\hat{\sigma}_y:\hat{\sigma}_x=1:0$.
 [+55/-55]_s-laminate, E-glass / MY750³;
 $b_{\perp}^{\tau}=1.5; b_{\parallel}=0.13; b_{\perp\parallel}^{\tau}=0.4, \hat{m}=3.1$,
 $\max \gamma = 4\%$. Eqn(45)

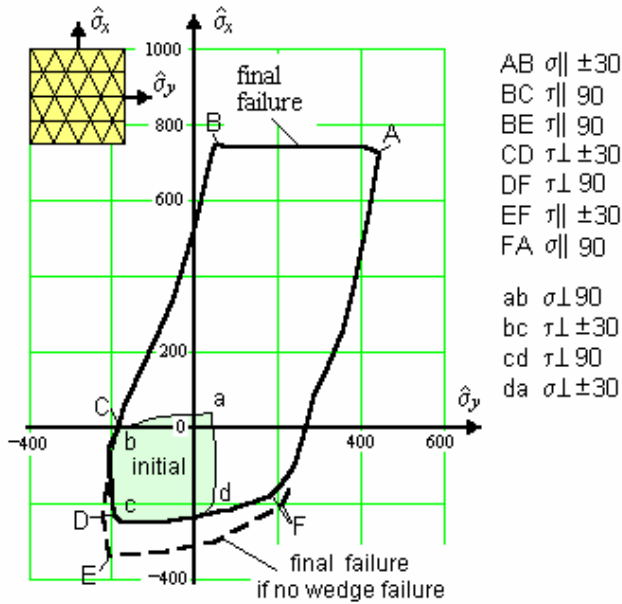


Fig. 26. Initial and final biaxial failure envel. $\hat{\sigma}_y(\hat{\sigma}_x)$
 [90/+30/-30]_s-laminate. E-glass / LY556 epoxy³.
 Eqn(45)

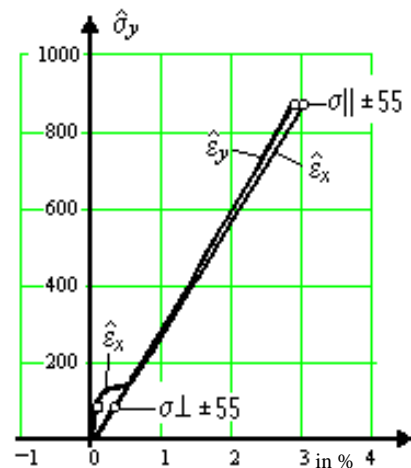


Fig. 28. Stress-strain curves $\sigma_y:\sigma_x=2:1$
 [+55/-55]_s-laminate. E-glass / MY750³

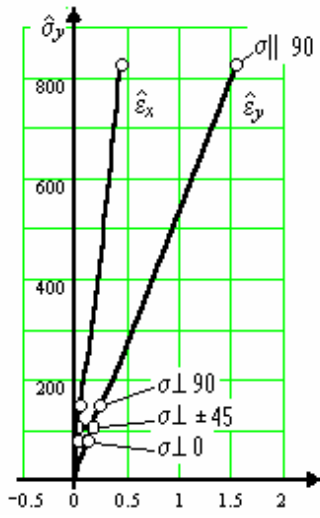


Fig. 29. Stress-strain curves $\hat{\sigma}_y:\hat{\sigma}_x = 2:1$.
 $[90/+45/-45/0]_s$ -laminate. AS4/3501-6 epoxy

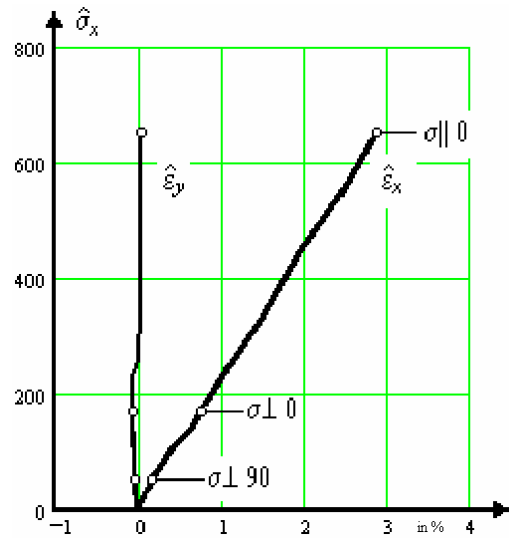


Fig. 31. Stress-strain curves $\sigma_y:\sigma_x=0:1$
 $[0/90]_s$ -laminate. E-glass / MY750³

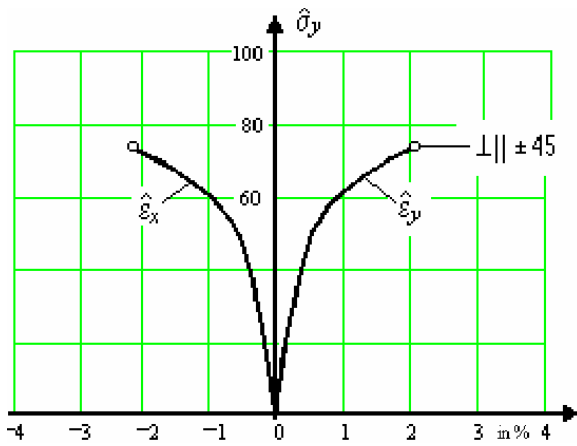


Fig. 30a. Stress-strain curves $\sigma_y:\sigma_x=1:-1$
 $[+45/-45]_s$ -laminate. E-glass / MY750³.
 (without temperature drop)

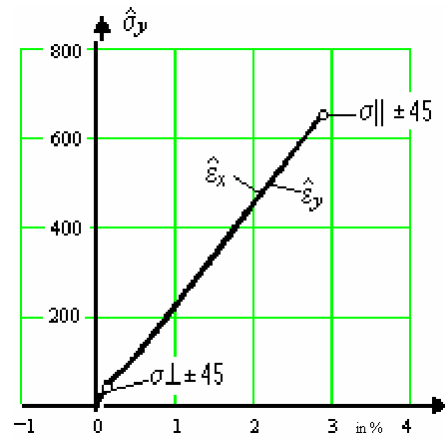


Fig. 32. Stress-strain curves $\sigma_y:\sigma_x=1:1$
 $[+45/-45]_s$ -laminate. E-glass / MY750³

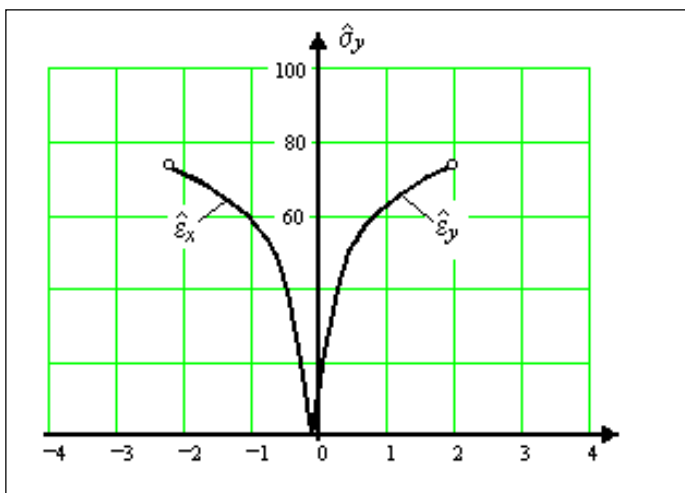


Fig. 30b. Stress-strain curves $\sigma_y:\sigma_x=1:-1$
 $[+45/-45]_s$ -laminate. E-glass / MY750³.
 (with temperature drop 100-200°C)

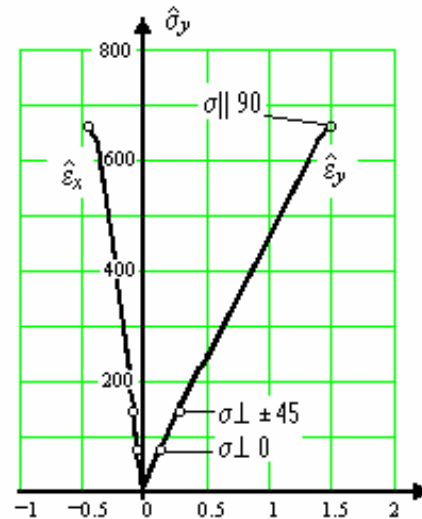


Fig. 33. Stress-strain curves $\sigma_y:\sigma_x=1:0$
 $[0/+45/-45/90]_s$ -laminate. AS4/3501-6 epoxy³

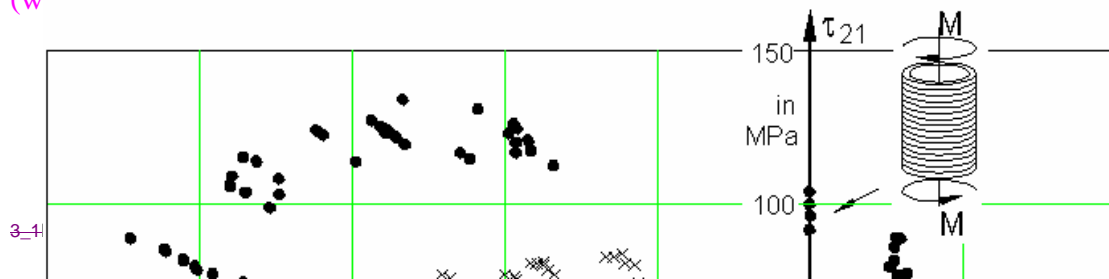


Table 1. Main features of the FMC

- Each *mode* represents one theoretically independent failure mechanism and one piece of the complete *failure surface* (surface of the failure body or *limit surface*)
- Each failure *mechanism* is represented by one failure *condition*. One failure mechanism is governed by one basic strength and therefore has a clearly defined equivalent stress σ_{eq}
- Curve-fitting of the course of test data is only permitted in the pure failure mode's regime
- Different, however, similar behaving materials obey the same function as failure condition but have *different curve parameters*
- Rounding-off in mode interaction zones is performed by a spring model.

Table 2. Additional FMC aspects/information

- An invariant formulation of a failure condition in order to achieve a *scalar* potential considering the material's symmetries (Chr97) is possible
- Each invariant term of the failure function shall be related to a physical mechanism observed in the solid, causing a volume change or a shape change or friction
- Hypotheses applied:
Hashin/Puck with Beltrami (choice of invariants), Mohr-Coulomb (friction, thinking in Mohr's stresses)
- The rounding-off of adjacent *mode failure curves* (*partial surfaces*) in their interaction zone is leading again to a *global failure curve* (surface) or to a 'single surface failure description' (such as with Tsai/Wu, however without the well-known shortcomings).
- * Proof of Design and *Strength* analysis:
 - For each *mode* one *reserve factor* $f_{Res}^{(mode)}$ or one stress effort (if nonlinear) is to be determined, displaying, where the design key has to be turned
 - The probabilistics-based 'rounding-off' approach delivers the *resultant reserve factor* linked to the *margin of safety* by $MS = f_{Res}^{(res)} - 1$.
- * *Nonlinear Stress* analysis with Degradation:
 - Equivalent stresses and stress efforts are used in this (nonlinear) progressive damage description.
 - Failure mode identification is mandatory for a progressive failure analysis in order to know how the lamina has failed. Criteria which just predict failure do not make a clear degradation of the moduli possible.

Table 3. Mechanical and thermal properties of the four UD-laminae of the 'failure exercise' [Sod98]

Fibre type	AS4	T300	E-glass 21xK43 Gevetex	Silenka Glass 1200tex	E-
Matrix	3501-6 ep.	BSL914C ep.	LY556/HT907	MY750/HY91	

Specification		Prepeg type Hercules	Filament wind. DFVLR	/ DY063 epoxy Filament wind. DLR	7/ DY063 epoxy Filament wind. DRA
Manufacturer Fibre	volume	fraction, 0.60	0.60	0.62	0.60
V_f					
Longitudinal $E_{ }$	modulus,	[GPa] 126a	138	53.48	45.6
Transverse E_{\perp}	modulus,	[GPa] 11	11	17.7	16.2
In-plane $G_{ \perp}$	shear modulus,	[GPa] 6.6a	5.5a	5.83a	5.83a
Major $\nu_{\perp }$	Poisson's ratio	0.28	0.28	0.278	0.278
Through thickness	Poisson's ratio	0.4	0.4	0.4	0.4
$\nu_{\perp\perp}$					
Longitudinal $R_{ }^t$	tensile strength	[MPa] 1950b	1500	1140	1280
Longitudinal [MPa] $R_{ }^c$	compressive strength,	1480	900	570	800
Transverse R_{\perp}^t	tensile strength,	[MPa] 48	27	35	40
Transverse R_{\perp}^c	compressive strength,	[MPa] 200b	200	114	145b
In-plane $R_{\perp }$	shear strength,	[MPa] 79b	80b	72b	73b
Longitudinal $e_{ }^t$	tensile failure strain, [%]	1.38	1.087	2.132	2.807
Longitudinal [%] $e_{ }^c$	compressive failure strain	1.175	0.652	1.065	1.754
Transverse e_{\perp}^t	tensile failure strain [%]	0.436	0.245	0.197	0.246
Transverse [%] e_{\perp}^c	compressive failure strain	2.0	1.818	0.644	1.2
In-plane $\gamma_{\perp }$	shear failure strain [%]	2	4	3.8	4
Strain energy G_{IC}	release rate, [Jm ⁻²]	220c	220	165	165
Longitudinal [10 ⁻¹ /°C] $\alpha_{ }$	thermal coefficient,	-1	-1	8.6	8.6
Transverse [10 ⁻² /°C] α_{\perp}	thermal coefficient,	26	26	26.4	26.4
Curing: Stress free temperature [°C]		177	120	120 2 h at 120°C 2 h at 150°C	120 2 h 90°C, 1.5 h
(Effective temperature difference [°C])		-125e	-68	-68	130°C, 2 h 150°C -68

^a Initial modulus. ^c Double cantilever specimen ^d assumption: linearized, reference temperature = RT = 22°C

^b Nonlinear behaviour, stress/strain curves and data points are provided ^e -177 + RT + 30 (moisture effect) = -125°C.

Temperature drop := Stress free temperature minus 22°C !

Table 4. Mechanical and thermal properties of the four fibres utilized[Sod98]

Fibre type			AS4	T300	E-glass 21 x K43, Gevetex	Silenka E-Gl. 1200tex
Longitudinal	modulus,	[GPa]	225	230	80	74
$E_{f }$						
Transverse	modulus,	[GPa]	15	15	80	74
$E_{f\perp}$						
In-plane	shear modulus,	[GPa]	15	15	33.33	30.8
$G_{f \perp}$						
Major	Poisson's ratio		0.2	0.2	0.2	0.2
$\nu_{f\perp }$						
Transverse	shear modulus	[GPa]	7	7	33.33	30.8
$G_{f \perp}$						
Longitudinal	tensile strength	[MPa]	3350	2500	2150	2150
$R_{f }^t$						
Longitudinal	compressive strength,	[MPa]	2500	2000	1450	1450
$R_{f }^c$						
Longitudinal	tensile failure strain, [%]		1.488	1.086	2.687	2.905
$e_{f }^t$						
Longitudinal	compressive failure strain [%]		1.111	0.869	1.813	1.959
$e_{f }^c$						
Longitudinal	thermal coefficient, [10 ⁻⁶ /°C]		-0.5	-0.7	4.9	4.9
$\alpha_{Mf }$						
Transverse	thermal coefficient, [10 ⁻⁶ /°C]		15	12	4.9	4.9
$\alpha_{Mf\perp}$						

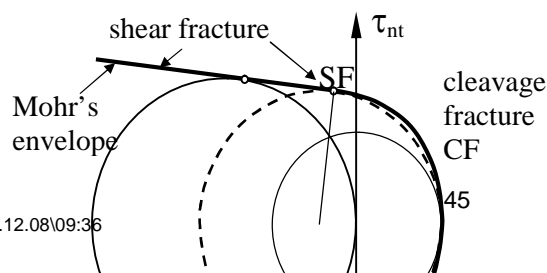
Table 5. Mechanical and thermal properties of the four matrices utilized [Sod98]

Matrix type			3501-6 ep.	BSL914C ep.	LY556/HT907 /DY063 epoxy	MY750/HY91 7/ DY063 epoxy
Manufacturer			Hercules	DFVLR	Ciba Geigy	Ciba Geigy
Longitudinal	modulus,	[GPa]	4.2	4.0	3.35	3.35
E_m						
In-plane	shear modulus,	[GPa]	1.567	1.481	1.24	1.24
G_m						
Major	Poisson's ratio		0.34	0.35	0.35	0.35
ν_m						
Longitudinal	tensile strength	[MPa]	69	75	80	80
R_m^t						
Longitudinal	compressive strength,	[MPa]	250	150	120	120
R_m^c						
In-plane	shear strength,	[MPa]	50	70	-	-
R_m^τ						
Longitudinal	tensile failure strain, [%]		1.7	4	5	5
e_m^t						

Longitudinal thermal coefficient, [10 ⁻⁴ 55 58 58 6/°C] α_{Tm}			
---	--	--	--

Table 6. Summary of laminate types, material types and plots required from contributors
($\hat{\sigma}_x = n_x / t$; $\hat{\sigma}_y = n_y / t$; t = laminate thickness)

Laminate type	Material type	Plots required and description of loading conditions
<ul style="list-style-type: none"> • 0° unidirectional lamina (isolated) 	<ul style="list-style-type: none"> E-glass/LY556/HT907/DY063 T300/BSL914C 	<ol style="list-style-type: none"> 1. σ_2 vs τ_{21} failure stress envelope 2. σ_1 vs τ_{21} failure stress envelope 3. σ_2 vs σ_1 failure stress envelope
<ul style="list-style-type: none"> • [90/+30/-30]_s laminate $t = 2.0$ mm, $t_{90} = 2 \cdot 0.172$, 	<ul style="list-style-type: none"> E-glass/LY556/HT907/DY063 	<ol style="list-style-type: none"> 4. $\hat{\sigma}_y$ vs $\hat{\sigma}_x$ failure stress envelope 5. $\hat{\sigma}_x$ vs $\hat{\tau}_{xy}$ failure stress envelope
<ul style="list-style-type: none"> • [90/45/-45/0]_s laminate $t = 1.1$ mm, $t_k = t / 8$ 	<ul style="list-style-type: none"> AS4/3501-6 (quasi-isotropic, widely used) 	<ol style="list-style-type: none"> 6. $\hat{\sigma}_y$ vs $\hat{\sigma}_x$ failure stress envelope 7. Stress/strain curves under uniaxial tensile loading for $\hat{\sigma}_y / \hat{\sigma}_x = 0/1$ 8. Stress/strain c. for $\hat{\sigma}_y / \hat{\sigma}_x = 2/1$
<ul style="list-style-type: none"> • [+55/-55]_s angle-ply laminate $t = 1.0$ mm, $t_k = t / 4$ 	<ul style="list-style-type: none"> E-glass/MY750/HY917/DY063 (piping, pressure vessels) 	<ol style="list-style-type: none"> 9. $\hat{\sigma}_y$ vs $\hat{\sigma}_x$ failure stress envelope 10. Stress/strain curves under uniaxial tensile loading $\hat{\sigma}_y / \hat{\sigma}_x = 0/1$ 11. Stress/strain c. for $\hat{\sigma}_y / \hat{\sigma}_x = 2/1$
<ul style="list-style-type: none"> • [0/90]_s cross-ply laminate $t = 1.04$ mm, $t_k = t / 4$ 	<ul style="list-style-type: none"> E-glass/MY750/HY917/DY063 	<ol style="list-style-type: none"> 12. Stress/strain curve under uniaxial tensile loading for $\hat{\sigma}_y / \hat{\sigma}_x = 0/1$
<ul style="list-style-type: none"> • [+45/-45]_s angle ply laminate $t = 1.0$ mm, $t_k = t / 4$ 	<ul style="list-style-type: none"> E-glass/MY750/HY917/DY063 	<ol style="list-style-type: none"> 13. Stress/strain c. for $\hat{\sigma}_y / \hat{\sigma}_x = 1/1$ 14. Stress/strain c. for $\hat{\sigma}_y / \hat{\sigma}_x = 1/-1$



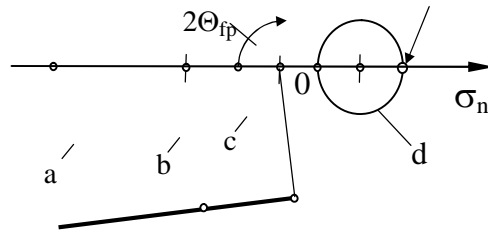
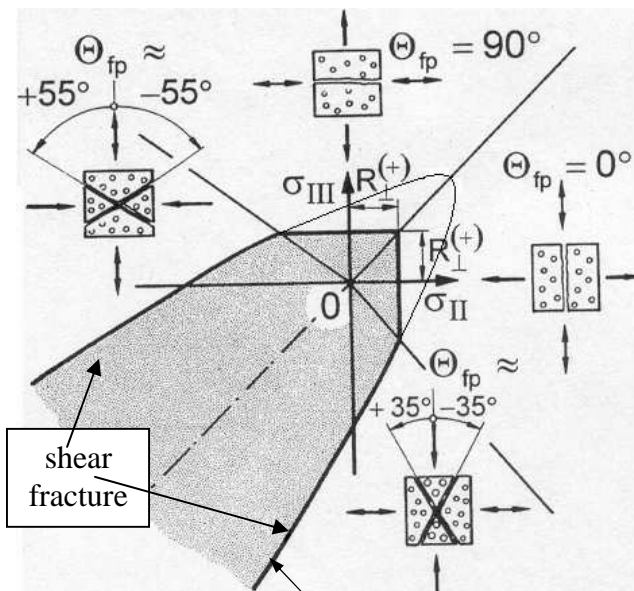
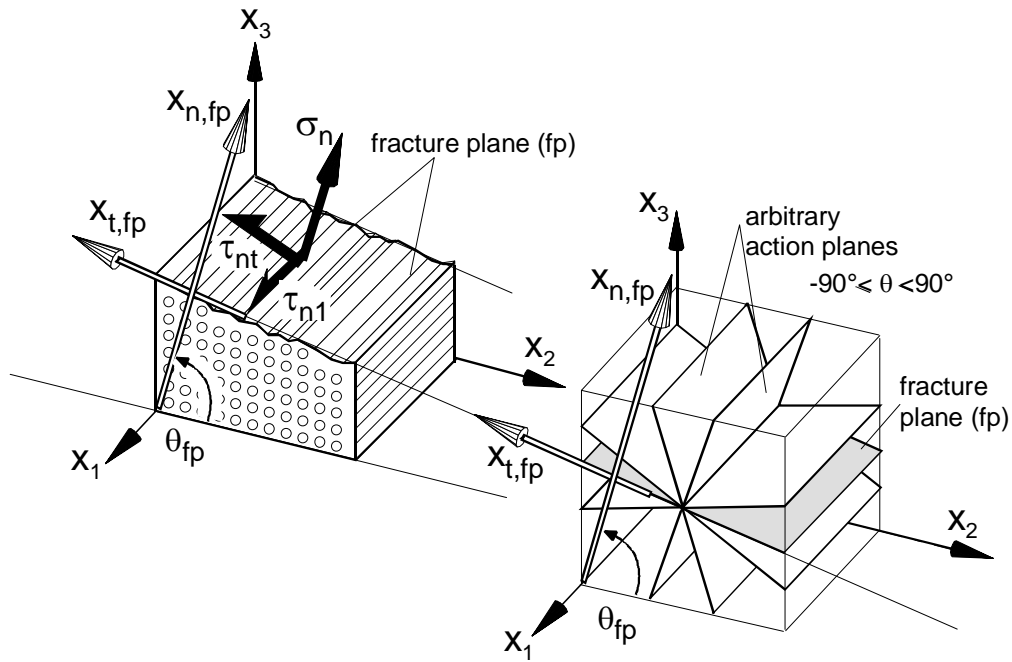


Figure A1/1. Mohr's fracture envelope and some Mohr circles for fracturing stresses
a) for uniaxial transverse compression σ_{II} ,
c) for pure shear $\tau_{23} = \sigma_{II} = -\sigma_{III}$,
d) for uniaxial transverse tension σ_{III} .
b) limiting circle for simultaneous shear fracture (SF) and cleavage fracture (CF) on different action planes. Between SF and CF no circle can touch the fracture envelope.



parabola according to eqn (A3)

Figure A1/2. Fracture curve (σ_{II} , σ_{III}) resulting from Fig. A1/1 with tensile cut-offs and typical fracture angles Θ_{fp} for uniaxial transverse tension and compression



$$\begin{Bmatrix} \sigma_n \\ \tau_{nt} \\ \tau_{n1} \end{Bmatrix} = \begin{bmatrix} c^2 & s^2 & 2sc & 0 & 0 \\ -sc & sc(c^2 - s^2) & 0 & 0 & 0 \\ 0 & 0 & 0 & s & c \end{bmatrix} \begin{Bmatrix} \sigma_2 \\ \sigma_3 \\ \tau_{23} \\ \tau_{31} \\ \tau_{21} \end{Bmatrix}$$

$c := \cos\theta,$
 $s := \sin\theta$

$\{\sigma^{\text{Mohr}}\} = (\sigma_n(\theta_{fp}), \tau_{nt}(\theta_{fp}), \tau_{n1}(\theta_{fp}))^T$

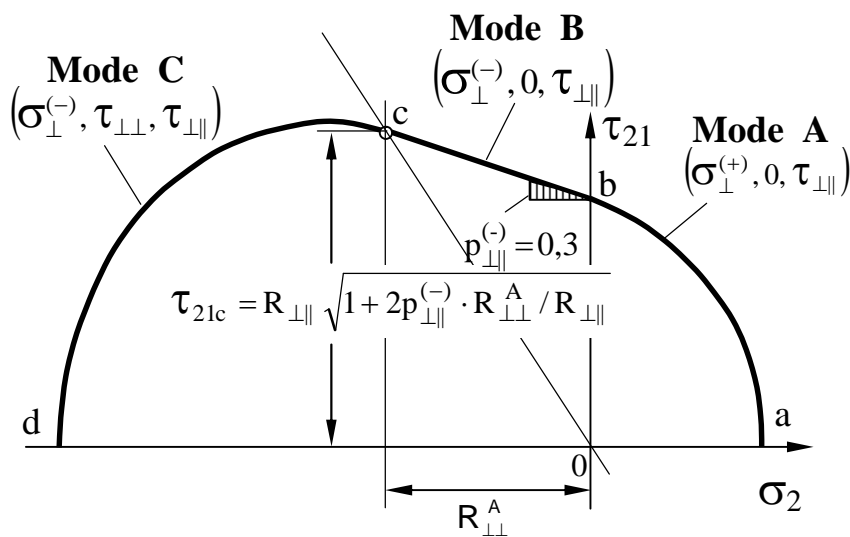


Figure A1/4. (σ_2, τ_{21}) - fracture curve with IFF-modes A, B, C

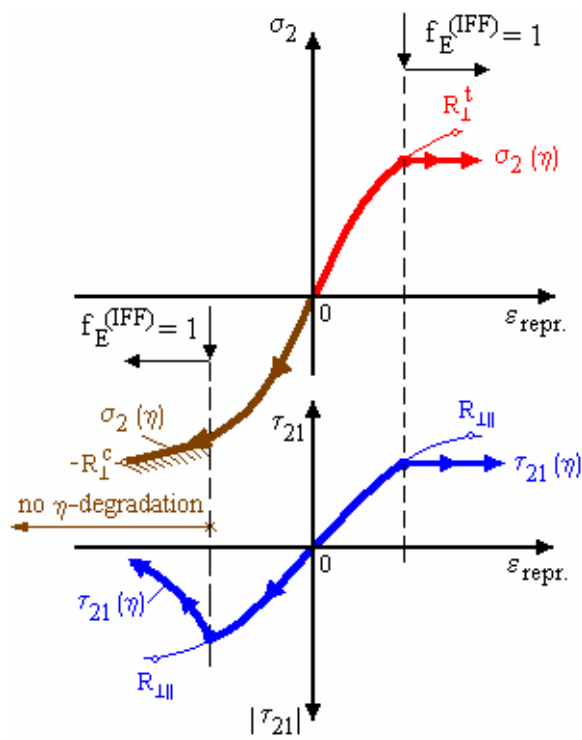


Fig. A1/5. Schematic illustration of Puck's assumptions about the average stresses $\sigma_2(\eta)$ and $\tau_{21}(\eta)$ after the onset of IFF. The strain $\varepsilon_{\text{repr.}}$ is a representative strain, which is proportional to the load on the laminate

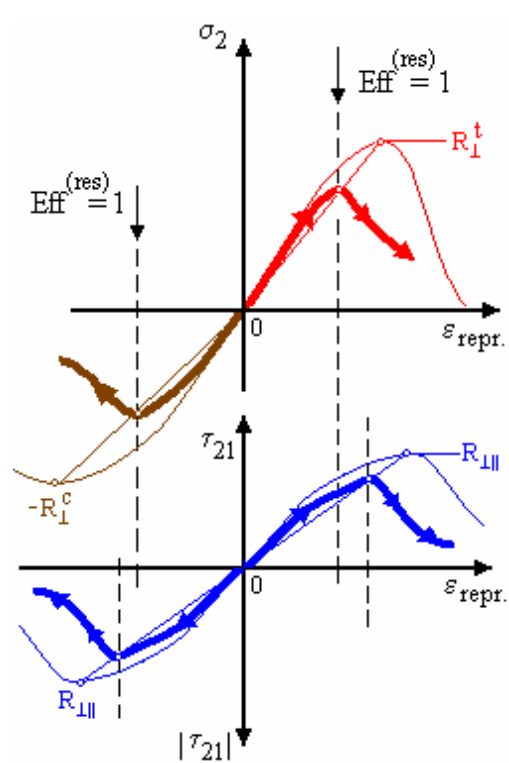


Fig. A1/6. Schematic illustration of Cuntze's assumptions about the stresses σ_2 and τ_{21} before and after IFF-initiation. Results of the 'triggering approach'.

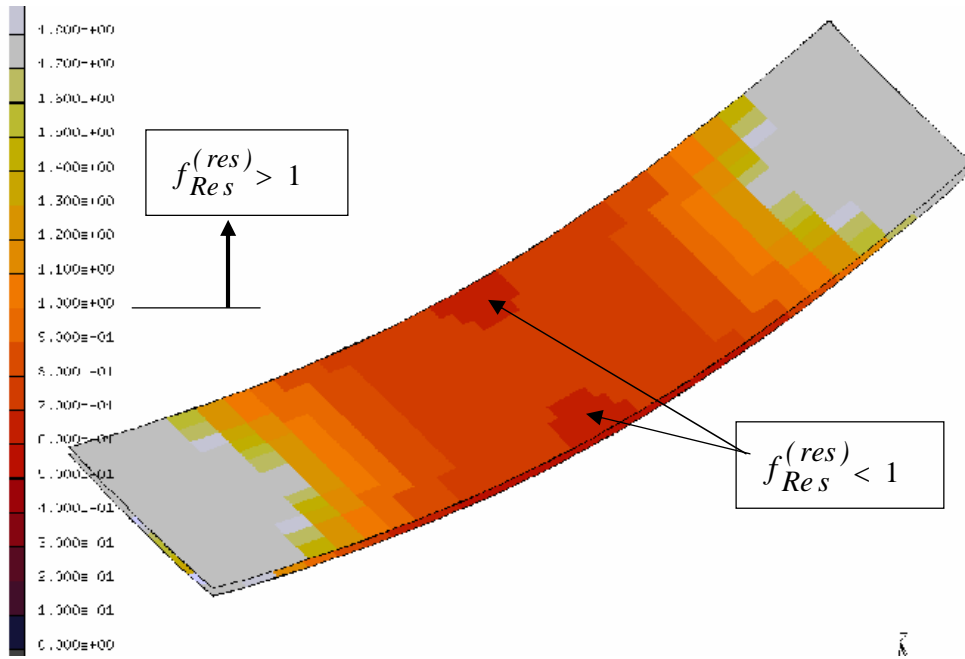
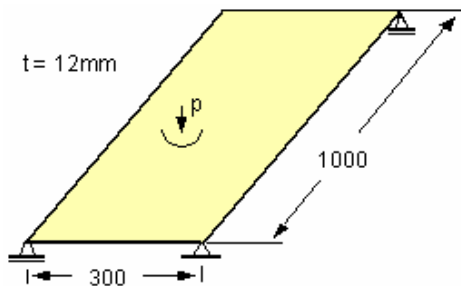


Figure A3/1: Reserve factor $f_{Res}^{(res)}$ of failure responsible lamina $k = 2$ (lower skin) [G. Sukarie, MARC]¹²

Table A3/1: Geometry and loads of the GFRP sandwich plate. Mechanical properties (mean values) and strength properties ($\nu_f = 0.60$) and data of calibration points (mean values)



- $\bar{R}_{||}^t$: Weibull, 1500 MPa, cov = 6 %
- $\bar{R}_{||}^c$: Weibull, 1200 MPa, cov = 7 %
- \bar{R}_{\perp}^t : Weibull, 40 MPa, cov = 12 %
- \bar{R}_{\perp}^c : Weibull, 144 MPa, cov = 7 %
- $\bar{R}_{\perp||}$: Weibull, 61 MPa, cov = 10 %

3D Volume FE model, analysis ply-by-ply,

- Face sheet: [0/45/90/-45/0], $t_{face} = 1$ mm each lamina from 0,2 mm tape
 - Core: 10 mm Rohacell R51
 - * Loads (no residual stresses): $p = 0,01$ MPa. Thickness: $1 + 10 + 1 = 12$ mm
- Volume finite elements; ply-by-ply analysis.

	GFRP	Rohacell R51
$E_{ }$	44500 MPa	$E = 60$ MPa
E_{\perp}	12500 MPa	-
$G_{ \perp}$	6000 MPa	$G = 25$ MPa
$\nu_{\perp }$	0.28	-
$\nu_{ \perp}$	0.40	-

Table A3/2. Reserve factors calculated for all laminae [G. Sukarie, MARC]¹²

		$f_{Res(k)}^{(res)}$	$f_{Res(k)}^{\sigma_{ }}$	$f_{Res(k)}^{\tau_{ }}$	$f_{Res(k)}^{\sigma_{\perp}}$	$f_{Res(k)}^{\tau_{\perp}}$	$f_{Res(k)}^{\perp_{ }}$
k = 1	0°:	1.33 [142]	12.8 [202]	100. [..1]	1.34 [142]	3.13 [141]	3.51 [142]
k = 2	45°:	0.87 [267]	27.6 [349]	53.3 [340]	0.893 [267]	1.75 [267]	2.26 [267]
k = 3	90°:	0.82 [686]	38.6 [574]	41.2 [606]	0.820 [686]	4.62 [559]	2.15 [686]
k = 4	-45°:	0.94 [750]	31.6 [821]	87.0 [762]	0.964 [750]	1.89 [766]	2.44 [750]
k = 5	0°:	1.92 [1146]	14.9 [996]	100. [961]	1.94 [1146]	5.21 [1146]	5.25 [1146]
k = 6	core:	Not relevant here					

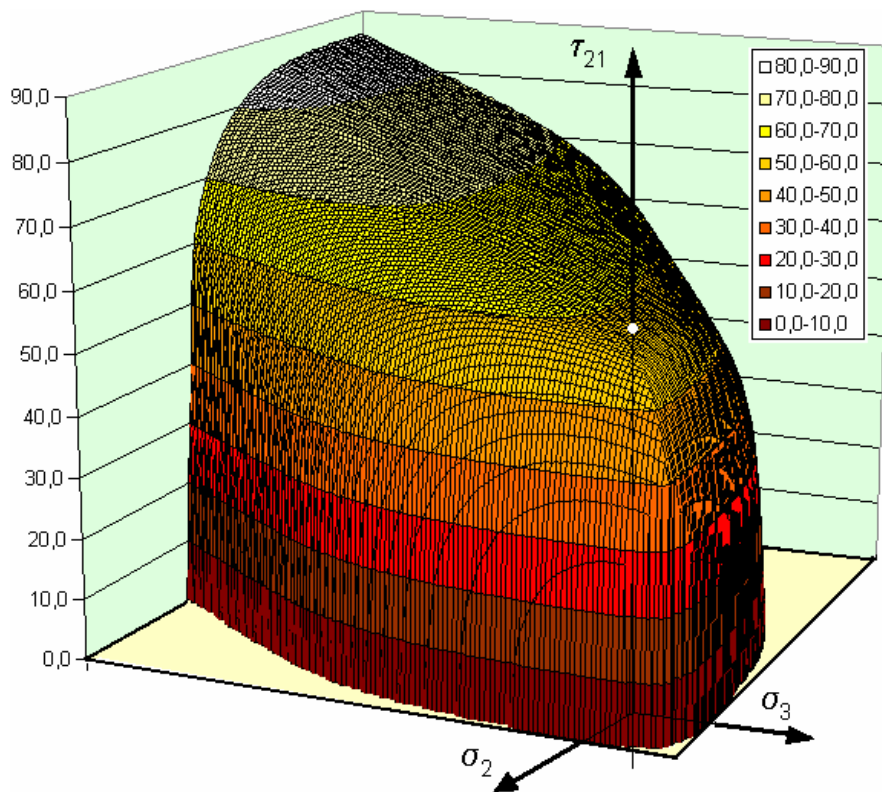


Figure 5. The $(\tau_{21}, \sigma_2, \sigma_3)$ - Failure Body

A1.2 Comparison of Puck's and Cuntze's laminate failure analysis

This section focusses on a 2D laminate failure analysis as performed in the Failure Analysis Exercise, Part. A.

For fibre failure (FF) both authors use the same simple maximum stress failure criteria.

$$-f_{E(FF)} = -\frac{\sigma_{1f}}{R_{\parallel}^t \cdot \varphi} = 1 \text{ for } \sigma_1 \geq 0 \text{ and } f_E = \frac{\sigma_1}{R_{\parallel}^c} = 1 \text{ for } \sigma_1 < 0 \quad (A6)$$

For this reason the predicted biaxial failure envelopes for final failure of laminates with 3 or more fibre directions, the strengths of which are fibre dominated, cannot differ very much. Also the stress/strain curves of these laminates predicted by both authors are looking likely very similar because the stiff fibres carry the main portion of the loads. Therefore different degradation procedures after the onset of interfibre failure (IFF) do not influence the predicted strains very much. This is especially true for CFRP laminates.

• Puck's degradation procedure after the onset of IFF (known as the η degradation) is rather simple because Puck's IFF criteria are completely mechanistic. For plane stress states ($\sigma_1, \sigma_2, \tau_{21}$) a numerical search for the fracture plane is not necessary because the fracture angle $\theta_{pf} = 0^\circ$ and for σ_2^t or moderate σ_2^c can be found analytically from

$$-\theta_{fp} = \arccos \frac{R_{\perp\perp}^A}{\sqrt{-\sigma_2^c}} \text{ for } \quad (A7)$$

high σ_2^c compressive stresses ($|\sigma_2^c| \geq R_{\perp\perp}^A$).

Therefore analytical solutions for the stress exposure factor $f_E^{(IFFmode)}$ could be found for 3 different domains of the stress σ_2 at fracture which shall be addressed as domains of the modes A, B, C:

$$-\text{for } \sigma_2 \geq 0 \quad f_E^{(modeA)} = \sqrt{\tau_{21}^2 + \left(\frac{R_{\perp\perp}}{R_{\perp}^t} - p_{\perp\parallel}^{(+)}\right)^2 \sigma_2^2 + p_{\perp\parallel}^{(+)} \sigma_2} \quad (A8)$$

Mode A combines the modes 1), 2), 3), 4) mentioned in (A?)

$$-\text{for } -R_{\perp\perp}^A \geq \sigma_2 < 0 \quad f_E^{(modeB)} = \frac{1}{R_{\perp\parallel}} \sqrt{\tau_{21}^2 + p_{\perp\parallel}^{(-)} \sigma_2^2 + p_{\perp\parallel}^{(-)} \sigma_2} \quad (A9)$$

Mode B is identical with mode 5)

$$-\text{for } R_{\perp}^c \leq \sigma_2 < R_{\perp\perp}^A \quad f_E^{(modeC)} = \frac{R_{\perp}^c}{4(R_{\perp\parallel} + p_{\perp\parallel}^{(-)} R_{\perp\perp}^A)^2} \cdot \frac{\tau_{21}^2}{(-\sigma_2)} + \frac{(-\sigma_2)}{R_{\perp}^c} \quad (A10)$$

Mode C combines modes 6) and 7).

In all three cases the fracture condition is given by

$$-f_E^{(IFFmode)} = 1. \quad (A11)$$

If in a loading process at a certain load level $f_E^{(IFFmode)} = 1$ is reached eg, for Mode A, this means that the onset of IFF ('cracking') is reached. Hence, the fracture angle θ_{pf} is 0° and as σ_2 is a tensile stress the cracks tend to open.

The resulting decrease of the secant moduli $E_{2(sec)}$ and $G_{21(sec)}$ is modelled by a simultaneously starting degradation of $E_{2(sec)}$ and $G_{21(sec)}$. That means secant moduli $\eta E_{2(sec)}$ and $\eta G_{21(sec)}$ with $\eta < 1$ are used after the onset of IFF. The degradation factor η is a decaying function decreasing with increasing load, so that the stress exposure factor $f_E^{(IFFmode)}$ is kept constant at 1 until final failure of the laminate. That means that also the 'average' stresses $\sigma_2(\eta)$ and $\tau_{21}(\eta)$ calculated with $\eta E_{1(sec)}$ and $\eta G_{21(sec)}$ respectively, are remaining

approximately constant after the onset of IFF (average stresses are defined: stresses sunearred over some length that includes IFF microcracks). [That means also that if both stresses σ_2 and τ_{21} are involved in producing the fracture, due to their interaction, the strengths $\sigma_2 = R^t$, and $\tau_{21} = R_{\perp\perp}$ are never reached (as within Cuntze's IFF interaction domains)].

In contrast to Puck's completely $f_{E(IFF)}$ -controlled η -degradation Cuntze uses the stress exposure factor $f_{E(IFF)}^{res}$ only for a certain correction in order to take Mode interactions into account. His degradation is mainly controlled by using the $\sigma_2(\epsilon_2)$ or $\tau_{21}(\gamma_{21})$ stress/strain curve, respectively, for the finding of the valid secant modulus E_{2s} or G_{21s} , respectively. The branches with increasing stresses (hardening) of these stress/strain curves are found by the usual experiments with uniaxial σ_2 -stress or pure τ_{21} -stress, respectively. The branches with rapidly decreasing stresses (called softening) are primarily assumed, see Figures 10 to 17. Like Puck/Cuntze calculates the stresses σ_2 and τ_{21} in the laminae of the laminate by using secant moduli from the $\sigma_2(\epsilon_2)$ and $\tau_{21}(\gamma_{21})$ stress/strain curves. However, because Cuntze's fracture conditions are formulated mainly in a probabilistic manner he has to take care for a proper interaction of the interactive modes in the stress and strain analysis in the following manner: In order to take the probabilistic and mechanistic interaction of the failure modes into account the secant moduli E_{2s} and G_{21s} are taken from the $\sigma_2(\epsilon_2)$ curve, better $\sigma_{eq}(\epsilon)$ curve because σ_{eq} may still include a τ_{21} -stress, or the $\tau_{21}(\gamma_{21})$ curve not just at the stresses $\sigma_{eq} = \sigma_2$ or τ_{21} , respectively, with the results from the stress and strain analysis for the given load, but at little higher stress in the 'hardening branch' with increasing stress and a little lower stress in the 'softening branch' with decreasing stress. This 'stress correction' is controlled by the so-called 'triggering approach', see eqns (35) and (36). The controlling parameter is the ratio of the resultant stress exposure factor $f_{E(IFF)}^{(res)}$ to the maximum mode exposure factor $\max f_E^{(IFF mode)}$. By this triggering approach a little lower secant moduli $E_{2(sec)}$ and $G_{21(sec)}$ are provided for the next calculation loop as those which would result directly from the stresses (IFF mode 1) $\sigma_{eq}^{\perp\sigma}$ or $\sigma_{eq}^{\perp\tau}$ and $\sigma_{eq}^{\perp\perp}$ (IFF mode Z) without the correction by the triggering approach. This shall take account of the degradation interaction.

In contrast to Puck's theory in Cuntze's theory the *triggered equivalent* stresses climb up to R_{\perp}^t or $R_{\perp\perp}$, of the associated (σ, ϵ) curve, respectively, before the secant moduli drop rapidly with increasing strain.

There is another difference: Cuntze's triggering approach has to be already active before the onset of IFF, while Puck's η -degradation starts just with the onset of IFF. A third difference becomes obvious if the number of strength properties is focussed: Puck very generally applies for each of the six basic states of stress $((\sigma_{\parallel}^t, \sigma_{\parallel}^c, \sigma_{\perp}^t, \sigma_{\perp}^c, \tau_{\perp\parallel}, \tau_{\perp\perp})$ one about the material behaviour, which is brittle in the actual case, he 'finds' a connection between the fracture resistance $R_{\perp\perp}$ and R_{\perp}^c .

Cuntze however, based on pre-information about the fracture morphology, directly applies the five strength $(R_{\parallel}^t, R_{\parallel}^c, R_{\perp}^t, R_{\perp}^c, R_{\perp\perp})$, only.

Another difference of the two theories, however, is the following: For a uniaxial compressive stress σ_2 Puck does not assume any η -degradation of the secant modulus $E_{2(sec)}$ because the (oblique) cracks caused by σ_2 keep closed. If Puck does not stop the calculation because of an assumed risk of delamination and local buckling due to the so-called wedge or explosion effect, the calculation is continued with an undegraded $E_{\perp(sec)}$ while Cuntze assumes a rapidly

~~decreasing σ_2^e stress with growing negative strain ϵ_2 if catastrophic failure of the delamination initiating wedge is prevented by the laminate.~~

~~Both authors are aware of the fact that up to now there is a serve lack of experimental experience about the 'real' degradation processes in FRP laminates. It is much to be hoped that the Failure Exercise and further research will promote knowledge in this field.~~

Table A1.1: Modelling of the (mean) strength failure body by mapping with suitable failure criteria models

—Interaction of stresses

Formulations of the failure criteria and strength failure modes for the UD lamina

In Cuntze's formulation just those stress interactions are included in the σ_{eq} which have an effect on the 'pure' IFF mode

—Interaction of the lamina's failure modes in the mode interaction zones

—Interaction of laminae in a laminate

Mechanistically considered by the strain controlling of the 0° lamina which is regarded by the application of the softening function and the η function.

Probabilistic aspects (see [Rae97], not yet investigated) round remaining corners according to the system reliability. The failure system laminate consists of the failure element laminae which are subjected to several strength failure modes.

Table A1.2: Modelling of the nonlinear laminate analysis by providing with clear, definitive values for the degrading elasticity properties of E_{11} , E_{22} , G_{12} , ν_{12} , ν_{21}